



Cite this: *Biomater. Sci.*, 2023, **11**, 6082

# Injectable hydrogels for the delivery of nanomaterials for cancer combinatorial photothermal therapy

Rita Lima-Sousa,<sup>a</sup> Cátia G. Alves,<sup>a</sup> Bruna L. Melo,<sup>a</sup> Francisco J. P. Costa,<sup>a</sup> Micaela Nave,<sup>a</sup> André F. Moreira,<sup>a</sup> António G. Mendonça,<sup>a,b</sup> Ilídio J. Correia<sup>a</sup> and Duarte de Melo-Diogo<sup>\*a</sup>

Progress in the nanotechnology field has led to the development of a new class of materials capable of producing a temperature increase triggered by near infrared light. These photothermal nanostructures have been extensively explored in the ablation of cancer cells. Nevertheless, the available data in the literature have exposed that systemically administered nanomaterials have a poor tumor-homing capacity, hindering their full therapeutic potential. This paradigm shift has propelled the development of new injectable hydrogels for the local delivery of nanomaterials aimed at cancer photothermal therapy. These hydrogels can be assembled at the tumor site after injection (*in situ* forming) or can undergo a gel–sol–gel transition during injection (shear-thinning/self-healing). Besides incorporating photothermal nanostructures, these injectable hydrogels can also incorporate or be combined with other agents, paving the way for an improved therapeutic outcome. This review analyses the application of injectable hydrogels for the local delivery of nanomaterials aimed at cancer photothermal therapy as well as their combination with photodynamic-, chemo-, immuno- and radio-therapies.

Received 16th May 2023,  
Accepted 17th July 2023  
DOI: 10.1039/d3bm00845b  
rsc.li/biomaterials-science

## 1. Introduction

Cancer is one of the leading causes of death worldwide, hence engaging much effort from the scientific community and industry.<sup>1,2</sup> To date, the intravenous administration of chemotherapeutic drugs (chemotherapy) has been the most widely applied therapeutic strategy for this disease.<sup>3</sup> However,

<sup>a</sup>CICS-UBI – Centro de Investigação em Ciências da Saúde, Universidade da Beira Interior, 6200-506 Covilhã, Portugal. E-mail: icorreia@ubi.pt, demelodiogo@ficsaude.ubi.pt; Fax: +351 275 329 099; Tel: +351 275 329 002  
<sup>b</sup>Departamento de Química, Universidade da Beira Interior, 6201-001 Covilhã, Portugal



Rita Lima-Sousa

Rita Lima-Sousa received her B.Sc. in Biochemistry and M.Sc. in Biomedical Sciences from the Universidade da Beira Interior in 2016 and 2018, respectively. Currently, Rita Lima-Sousa is a Ph.D. student in Biochemistry at the same university (with a Ph.D. scholarship awarded by FCT) and is developing her thesis in Prof. Ilídio J. Correia's group. Her research interests are focused on the development and functionalization of graphene

family nanomaterials and injectable hydrogels for application in cancer photothermal therapy and biomedicine.



Ilídio J. Correia

Ilídio J. Correia is a Full Professor in the department of Health Sciences at the Universidade da Beira Interior. He obtained his B.Sc. and Ph.D. degrees in Biochemistry from the University of Lisbon in 1998 and the New University of Lisbon in 2003, respectively. His research group is involved in the development of skin and bone substitutes, drug delivery systems, as well as in vitro 3D cell culture models of cancer.



this route has some severe side effects associated with its non-specificity towards cancer cells, ultimately leading to systemic toxicity.<sup>3</sup> To overcome such constraints, the cancer research community has been focused on developing new therapeutic weapons.<sup>4–7</sup>

A more up-to-date anticancer strategy that is currently under investigation relies on the use of nanomaterials-mediated photothermal therapy (PTT).<sup>8–11</sup> In this approach, nanostructures with photoresponsiveness are administered intravenously, accumulate at the tumor site and, upon irradiation with near infrared (NIR, 750–1000 nm) light, produce a local temperature increase, resulting in the death of cancer cells.<sup>12–14</sup> Considering that NIR radiation minimally interacts with biological components (*e.g.*, water, melanin), its use is crucial for achieving a high penetration depth and negligible off-target heating.<sup>12</sup> Hence, PTT mediated by nanomaterials may allow accurate spatio-temporally controlled treatment.<sup>15</sup> Inorganic nanostructures such as anisotropic gold nanoparticles (*e.g.*, gold nanorods,<sup>16</sup> gold nanostars<sup>17</sup>), carbon-based nanomaterials (*e.g.*, carbon nanotubes,<sup>18</sup> graphene oxide (GO),<sup>19</sup> reduced graphene oxide (rGO)<sup>20</sup>), or transition metal dichalcogenides (*e.g.*, MoS<sub>2</sub><sup>21</sup> and WS<sub>2</sub> nanosheets<sup>22</sup>) have been employed for cancer PTT due to their high NIR absorption and photothermal capacity. In turn, NIR-absorbing small molecules (*e.g.*, indocyanine green (ICG),<sup>23</sup> IR780,<sup>24</sup> IR820<sup>25</sup>) have been loaded into nanostructures due to their multimodal character and biodegradability, being promising nanoagents for cancer PTT. Such small molecule-based photothermal agents may also be covalently modified (*e.g.*, with polymers, amino acids) to generate self-assembling nanostructures intended for cancer PTT.<sup>26,27</sup>

Notwithstanding the nanoparticles' anticancer potential, their translation to the clinic has been slow. Nanomaterials administered systemically (*i.e.*, by intravenous injection) rely heavily on the differently sized fenestrae of tumor vasculature to passively accumulate at the tumor zone (enhanced per-

meability and retention (EPR) effect).<sup>28,29</sup> However, only a very small portion of the intravenously administered nanoparticles reaches the tumor site (less than 1% (median)).<sup>30</sup> Besides this, the models currently available for the pre-clinical screening of nanomaterials also show an exaggerated EPR effect.<sup>31</sup> In fact, the EPR effect is not ubiquitously present on human solid tumors, which further hinders nanomaterials' translation.<sup>31,32</sup>

In order to benefit from the potential of nanomaterials-mediated PTT, it is crucial to overcome their systemic administration-related issues. In this regard, the incorporation of nanomaterials into macroscale systems (*e.g.*, microneedles, injectable hydrogels, scaffolds) has been receiving great attention.<sup>33–35</sup> These macroscale systems can be locally injected/implanted into the tumor zone, thus sustaining the delivery of the nanoparticles into the diseased site.<sup>36</sup> Moreover, this approach can maximize the accumulation of nanoparticles in the tumor as well as reduce their leakage to adjacent tissues, avoiding possible side effects.<sup>36</sup> Among the different types of macroscale systems, injectable hydrogels have received great interest due to their unique set of properties.<sup>37,38</sup>

These injectable hydrogels have a straightforward formulation and can be assembled at the tumor site (*in situ*-forming hydrogels) or can undergo a gel-sol-gel transition during injection (shear-thinning/self-healing hydrogels).<sup>37,39,40</sup> In this way, these can be administered through a minimally invasive procedure and can reach deeper tumors when compared with microneedle patches.<sup>41,42</sup> Besides coordinating the delivery of the NIR light-responsive nanoparticles directly into the tumor site, the hydrophilic network of the hydrogels can also incorporate other agents (*e.g.*, drugs, immunostimulants), opening a venue for combinatorial PTT approaches.<sup>43,44</sup> For instance, Huang *et al.* compared the biodistribution of doxorubicin (DOX) and DOX-loaded nanoparticles (both administered by intravenous injection) with that attained using an injectable hydrogel containing DOX-loaded nanoparticles (by peritumoral injection).<sup>45</sup> The free DOX and DOX-loaded nanoparticles achieved tumor uptake, but their concentration at this site decreased after 1 day. In turn, the injectable hydrogel containing the DOX-loaded nanoparticles promoted a higher tumor accumulation of this agent (at least for 21 days) with minimal distribution to off-target organs (*e.g.*, liver, spleen, lungs). In fact, several studies have demonstrated that the delivery of nanostructures (or drugs) using injectable hydrogels results in a prolonged tumor uptake and/or minimal off-target accumulation.<sup>46,47</sup> Depending on the components used for their production, the injectable hydrogels also display good physical and chemical properties, biodegradability, and biocompatibility.<sup>34</sup>

In this review, the application of injectable hydrogels for the local delivery of nanoparticles aimed at cancer PTT as well as their potential for combinatorial PTT is analyzed. Firstly, an overview of the properties and capabilities of injectable hydrogels designed for tumor-confined delivery of nanomaterials will be provided (section 2). Afterwards, the application of injectable hydrogels for guiding nanomaterials-mediated PTT



**Duarte de Melo-Diogo**

*Duarte de Melo-Diogo received his B.Sc. and M.Sc. degrees in Biomedical Sciences from the Universidade da Beira Interior (UBI) in 2012 and 2014, respectively. In 2018, Duarte de Melo-Diogo received his Ph.D. degree in Biochemistry from the same university. Currently, he is an Invited Assistant Professor at UBI and Junior Researcher at the Centro de Investigação em Ciências da Saúde (CICS-UBI). His research interests are*

*focused on the biomedical application of graphene family nanomaterials, production of functional nanostructures for cancer therapy and development of macroscale delivery systems.*



will be analyzed (section 3). Then, the use of injectable hydrogels for nanomaterials-mediated PTT in synergy with other therapeutic modalities (photodynamic-, chemo-, immuno- and radio-therapies) will be discussed (section 4). Finally, an outlook regarding the state-of-the-art and future directions is provided (section 5). For the sake of brevity, this review will be focused on hydrogels for cancer combinatorial-PTT that are locally administered by intratumoral/peritumoral injections.

## 2. Overview of injectable hydrogels for the delivery of nanomaterials for cancer PTT

Injectable hydrogels allow local nanoparticle delivery in a relatively non-invasive manner (*i.e.*, through injection) when compared with their implantable equivalents.<sup>48–50</sup> This can greatly reduce discomfort and risk of infection.<sup>49,50</sup>

In general, two main types of injectable hydrogels have been used for the delivery of nanoparticles aimed at cancer PTT: injectable *in situ*-forming hydrogels and shear-thinning/self-healing hydrogels.<sup>37,39,40</sup> Regarding the former, as their name states, these are formed *in situ* (*i.e.*, at the tumor site). In brief, the procedure for injectable *in situ*-forming hydrogel administration is based on the loading of precursor solutions (polymeric solutions and/or crosslinking agents) and NIR-responsive nanoparticles into a syringe.<sup>43,44,48,51</sup> This mixture is then administered at the tumor site, allowing the hydrogel formation *in situ* by a crosslinking reaction, the nanoparticles being entrapped within the polymeric structure.<sup>6</sup> Thus, the hydrogel should have a fast gelation time to prevent premature leakage of the therapeutic nano-agents.<sup>52</sup> At the same time, the hydrogel must also allow the sustained release of the entrapped molecules.<sup>53</sup> Then, the tumor area is irradiated with a NIR light, and an on-demand temperature increase occurs after the nanomaterials' interaction with this radiation.

In the case of shear-thinning/self-healing hydrogels, these are pre-formed in the syringe.<sup>54</sup> Upon injection at the tumor site, the generated shear force allows the dissociation of the crosslinking bonds, and the hydrogel extravasates through the needle due to a decrease in its viscosity.<sup>54,55</sup> When this force is no longer applied, the crosslinking interactions are rebuilt (self-healing) and the hydrogel network is restored at the tumor site.<sup>54,55</sup> Afterwards, the nanomaterials' PTT can be initiated with the irradiation of the tumor zone with NIR light. This type of hydrogel allows for a more homogeneous encapsulation of the nanomaterials, injection without clogging and controlled release of the payload.<sup>55</sup>

### 2.1. Crosslinking mechanisms

Injectable hydrogels can be classified according to their crosslinking mechanism.<sup>48,53</sup> Chemically crosslinked hydrogels are formed by covalent bonds between the polymeric components and are characterized by higher mechanical strength and physical stability, giving them a prolonged degradation time.<sup>6</sup>

It should be noted that some chemical reactions may require the assistance of additional agents such as photoinitiators, catalyzers, or organic solvents, demanding special attention to ensure the hydrogel's biocompatibility.<sup>6,56</sup> The typical reactions in chemically crosslinked injectable hydrogels are (i) Schiff base reactions between an amine and carbonyl-containing aldehyde/ketone; (ii) Michael addition reactions where there is a nucleophilic addition to an unsaturated carbonyl compound, like  $\alpha,\beta$ -unsaturated carbonyl; (iii) disulfide bond formation between peripheral thiol groups; (iv) Diels–Alder “click” reaction between a conjugated diene and an alkene/alkyne; (v) polymerization in the presence of a photoinitiator; and (vi) azide–alkyne cycloaddition between these two functional groups, with Cu(I) as a catalyst (Fig. 1).<sup>6,48,57–63</sup>

Physically crosslinked hydrogels are formed by non-covalent interactions, displaying excellent injectability and biocompatibility.<sup>6</sup> However, these types of hydrogels tend to have a relatively low mechanical strength.<sup>40,48</sup> The typical reactions in physically crosslinked hydrogels are (i) hydrophobic interactions between hydrophobic segments that result in aggregation in aqueous solutions; (ii) hydrogen bonding between hydrogen atoms in highly electronegative groups and other electronegative atoms; (iii) ionic crosslinking formed by electrostatic forces between two oppositely charged molecules; (iv) host–guest interactions between a host molecule that includes/complexes a guest molecule in their structure; and (v)  $\pi$ – $\pi$  interactions between the aromatic ring of two molecules rich and short of electrons (Fig. 1).<sup>6,48,51,64–69</sup>

### 2.2. Stimuli-responsiveness

Injectable hydrogels can also be engineered to be sensitive to external or internal (*i.e.*, endogenous) stimuli.<sup>70–72</sup> This responsiveness can be applied in triggering the hydrogels' assembly/disassembly at the tumor site, their degradation, and in the release of the incorporated nanomaterials.<sup>71,73</sup>

Regarding external stimuli, injectable hydrogels can, for example, be light-responsive (*e.g.*, UV or NIR light).<sup>74–76</sup> The application of light may (i) induce the photopolymerization or photooxidation of crosslinking bonds mediated by the initiator; (ii) cause photoisomerization; or (iii) generate a temperature increase (mediated by the loaded photothermal agents) that alters the hydrogel's solid form.<sup>71,77,78</sup> This photo-induced heat can also be used to induce a controlled release of nanotherapeutic agents.<sup>51</sup> For instance, Wang and co-workers prepared a light-responsive hydrogel using methacrylic anhydride-modified chitosan and poly(*N*-isopropylacrylamide) (PNIPAM) that incorporated carbon-based nanostructures and DOX.<sup>79</sup> The combination of irgacure 2959 (photoinitiator) and UV light triggered a photocrosslinking process between the methacrylic groups that led to the hydrogel's assembly. In turn, the photothermal effect induced by the carbon-based nanostructures after NIR irradiation induced the shrinking of the hydrogel (behavior attributed to PNIPAM) and triggered the DOX release.<sup>79</sup>

Moreover, by incorporating superparamagnetic nanostructures (*e.g.*, Fe<sub>3</sub>O<sub>4</sub> nanoparticles) into the injectable hydro-



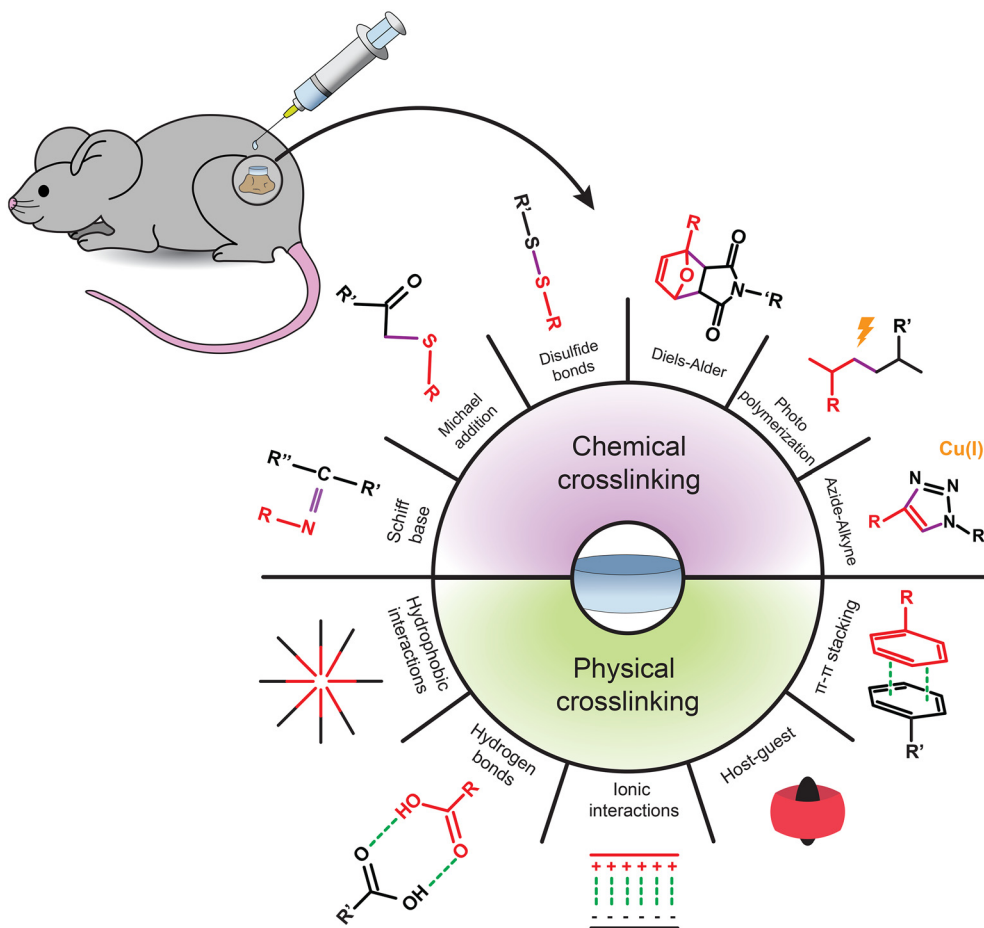


Fig. 1 Schematic illustration of the chemical and physical crosslinking methods used for the assembly of injectable hydrogels.

gels, it is possible to attain responsiveness to magnetic fields.<sup>56,80</sup> The interaction of these nanostructures with the magnetic field can also produce a local temperature increase that can change the hydrogel's properties (*e.g.*, increasing the drug release).<sup>80</sup>

Concerning internal/endogenous stimuli, injectable hydrogels can be engineered to be responsive to body temperature.<sup>81,82</sup> Moreover, the tumor microenvironment also displays a set of characteristics that can be used as internal/endogenous stimuli (lower pH or overexpression of specific enzymes (*e.g.*, matrix metalloproteinases (MMPs))).<sup>70</sup>

There can be two types of temperature-responsiveness: injectable hydrogels' viscosity can decrease or augment with the temperature increase.<sup>44,72,83</sup> The former can be helpful in terms of release of loaded therapeutic agents, whereas the latter is more advantageous for efficient gelation in the tumor area. One popular strategy explores the use of polymeric formulations that present a low viscosity at room temperature (to make injection easier) and then, after injection in the tumor zone, undergo a sol-to-gel transition at body temperature.<sup>66,83,84</sup> The best-known polymers with thermal responsiveness include the Pluronic family, cellulose, chitosan, or agarose derivatives.<sup>84</sup> For example, Zheng *et al.* devel-

oped a temperature-responsive hydrogel composed of chitosan and  $\beta$ -glycerophosphate incorporating DOX and poly(ethylene glycol) (PEG)-functionalized  $\text{MoS}_2/\text{Bi}_2\text{S}_3$  nanosheets for cancer therapy.<sup>85</sup> Upon mixing, these components could be loaded into a syringe and easily extruded. This formulation gellified at 37 °C due to a combination of hydrogen bonding and electrostatic and hydrophobic interactions between chitosan and  $\beta$ -glycerophosphate.<sup>85</sup>

Regarding pH-responsive injectable hydrogels, one possible approach explores crosslinking bonds that are stable at physiological pH but suffer rapid breakdown in the acidic conditions found within the tumor extracellular fluid.<sup>34,86</sup> Qu and colleagues developed an injectable hydrogel based on the covalent and pH-sensitive Schiff base bond between *N*-carboxyethyl chitosan (CEC) and dibenzaldehyde-terminated PEG (PEG-DA) for the intratumoral delivery of DOX.<sup>87</sup> At the mildly acidic tumor pH, the primary amine groups of CEC become positively charged, weakening the Schiff base crosslinking. Such change promoted the hydrogel's degradation and accelerated the release of the loaded cargo.<sup>87</sup>

Enzyme-responsive hydrogels aim to take advantage of enzymes overexpressed at the tumor site.<sup>53</sup> For instance, the tumor microenvironment has high amounts of MMPs that





degrade the basement membrane and extracellular matrix, playing an important role in several cancer processes.<sup>88</sup> Generally, the preparation of enzyme-responsive hydrogels is based on the incorporation of enzyme-cleavable crosslinkers (e.g., short peptides<sup>89</sup>) and enzyme-cleavable polysaccharides (e.g., hyaluronic acid (HA) since it is degraded by hyaluronidase<sup>90</sup>). Li *et al.* developed an enzyme-responsive injectable hydrogel formulated through Michael addition reactions between acrylated-HA and cysteine-modified peptides containing an MMP-2-cleavable sequence (GPQGIWGQ), that also incorporated DOX-loaded micelles.<sup>91</sup> In the presence of MMP-2, this hydrogel promoted a 1.45-times greater DOX release than in the absence of MMP-2.

### 3. Injectable hydrogels for cancer PTT

Injectable hydrogels can incorporate NIR-responsive nanomaterials into their hydrophilic structure, protecting them from degradation and sustaining their tumor-confined delivery.<sup>43</sup> In this way, injectable hydrogels have been explored for the local delivery of nanomaterials aimed at cancer PTT (Table 1) (Fig. 2A–D).

When the radiation interacts with the photothermal nano-agent incorporated into the tumor-confined hydrogel, it is absorbed, and the energy is released as heat.<sup>43</sup> If the final temperature at the tumor site is around 41–45 °C there can be (i) changes in cells' metabolic functions, (ii) inhibition of the DNA repair mechanisms, (iii) increase in the blood flow at the tumor site, (iv) increase in the oxidative stress and formation of reactive oxygen species (ROS), (v) a rise in the infiltrated immune cells, and (vi) sensitization of cells to the action of other therapies.<sup>8,92–95</sup> However, these effects are sublethal and can be reversible. On the other hand, local temperature increases to about 50 °C (or above) induce permanent damage: (i) the cell membrane collapses, (ii) the proteins denature, and (iii) the enzymatic and mitochondrial functions are rendered dysfunctional.<sup>13,94,96</sup> Such effects are non-reversible and ultimately lead to cell death by necrosis.<sup>97,98</sup> The cellular and molecular mechanisms prompted by these photothermally induced events have been extensively reviewed elsewhere.<sup>99–103</sup>

Additionally, the temperature increase that occurs during irradiation can also affect the structure of thermosensitive hydrogels (discussed in section 2). CuS nanodots, polydopamine (PDA) nanostructures, gold-based nano-systems, GO derivatives, ICG and IR820 are some NIR-responsive agents that have been incorporated into injectable hydrogels intended for cancer PTT.<sup>104–110</sup>

He and co-workers developed an injectable hydrogel composed of silk fibroin that incorporated GO complexed with upconversion nanoparticles (UCNP).<sup>111</sup> This hydrogel was formed through hydrophobic interactions that changed the silk fibroin from a random coil structure to the more stable  $\beta$ -sheet conformation.<sup>112</sup> In this system, UCNP were used as imaging agents (upon excitation with 980 nm light) while GO

acted as photothermal agent (upon exposure to 808 nm radiation).<sup>111</sup> After administration of the macroscale formulation into the breast tumor of mice and *in situ* gelation, this area was irradiated with 808 nm light ( $1 \text{ W cm}^{-2}$ , 5 min), reaching a temperature increase to about 57 °C that resulted in potent tumor regression.<sup>111</sup>

In another work, Cao *et al.* developed a poly(D,L-lactic acid-co-glycolic acid)-*b*-PEG-*b*-poly(D,L-lactic acid-co-glycolic acid)-based injectable hydrogel incorporating ancient ink nanoparticles as the PTT agent for colon cancer therapy.<sup>113</sup> This injectable hydrogel displayed a thermo-responsive assembly, achieving gelation when the temperature increased from 25 °C to 37 °C (physiological temperature). When the administered injectable hydrogel was subjected to NIR light (1064 nm,  $0.5 \text{ W cm}^{-2}$ , 15 min), it could produce a temperature increase to approximately 48.7 °C, resulting in a tumor growth reduction of about 84%.<sup>113</sup>

### 4. Injectable hydrogels for cancer combinatorial therapy

Injectable hydrogels can also be used for the local co-delivery of photothermal nanostructures and other therapeutic agents.<sup>37,56</sup> This combinatorial approach opens a venue for exploring the strong aspects of each therapeutic regimen, possibly leading to synergistic effects (Table 2).<sup>72,127</sup> This can also lead to a reduction of the required NIR laser and nanoparticle doses. This type of combinatorial therapy mediated by the injectable hydrogels is also important to achieve a greater therapeutic outcome, especially when the standalone PTT is not capable of destroying the residual cancer cells.

#### 4.1. Injectable hydrogels for cancer photodynamic-PTT

Injectable hydrogels that incorporate photothermal nanoagents and photosensitizers have triggered the interest of researchers (Table 2). Upon interaction with laser light, the photosensitizers are able to create ROS such as singlet oxygen, hydrogen peroxide, superoxide anion and hydroxyl radicals (photodynamic therapy (PDT)) (Fig. 2E–H).<sup>128</sup> At suitable levels, these ROS are extremely toxic to cancer cells since these can (i) affect the DNA and the permeabilization of the mitochondria's outer membrane, (ii) cause damage to the tumor vasculature, and (iii) induce an inflammatory response.<sup>129–131</sup> Interestingly, the ROS produced during PDT can also act as initiators in the photopolymerization/photocrosslinking of some injectable hydrogels.<sup>132</sup> To date, different photosensitizers (e.g., IR780,<sup>51</sup> ICG,<sup>133</sup> Ce6<sup>134</sup>) have been incorporated into injectable hydrogels aimed at cancer therapy, either dispersed in the gels' hydrophilic network or encapsulated within the nanomaterials.

Besides the standalone effects of the nanomaterials' PTT (described in section 3) and those from PDT (described above), each regimen can potentiate the other, making injectable hydrogels for combinatorial photodynamic-PTT very appealing. On one hand, photothermal heating can increase the blood

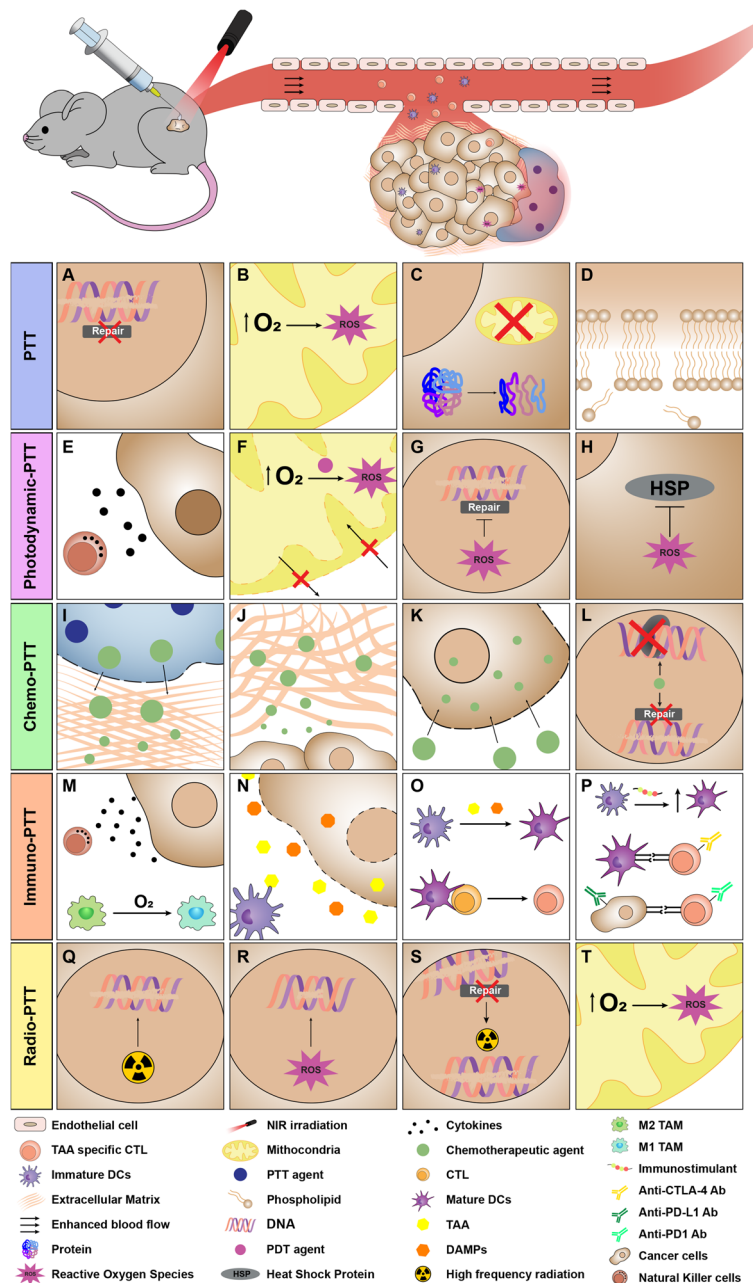


Table 1 Injectable hydrogels for PTT mediated by nanomaterials

| Hydrogel components   | Modality | Tumor model                   | Administration route | Hydrogel volume                                   | Laser parameters   | Therapeutic outcome   | Ref. |
|---|----------|-------------------------------|----------------------|---|--|---|------|
| MnO <sub>2</sub> nanoparticles and PND <sup>a</sup> hydrogel  | PTT      | 4T1 tumor-bearing mice        | i.t. <sup>b</sup>    | 50 $\mu$ L  | 808 nm, 0.8 W cm <sup>-2</sup> , 5 min (day 0 and day 7)                           | Primary tumor eradication<br>Secondary tumor growth reduction | 104  |
| MnO <sub>2</sub> nanoparticles and PND hydrogel   | PTT      | 4T1 tumor-bearing mice        | i.t.                 | 50 $\mu$ L  | 808 nm, 1 W cm <sup>-2</sup> , 5 min (day 0 and day 5)                             | Re-inoculated tumor growth reduction                          | 104  |
| Carbon particles incorporated into chitosan, HA and $\beta$ -sodium glycerophosphate hydrogel   | PTT      | MNNG/HOS tumor-bearing mice   | i.t.                 | 50 $\mu$ L  | 808 nm, 0.52 W cm <sup>-2</sup> , 10 min   | Tumor eradication   | 114  |
| PLGA <sup>c</sup> microspheres and IR820 incorporated into methylcellulose hydrogel   | PTT      | 4T1 tumor-bearing mice        | p.t. <sup>d</sup>    | —   | 808 nm, 1 W cm <sup>-2</sup> , 5 min   | Tumor eradication (3 out of 4)                                | 115  |
| Au-polyetherimide-UCNP <sup>e</sup> and smDNA <sup>f</sup> hydrogel   | PTT      | T24 tumor-bearing mice        | s.c. <sup>g</sup>    | 100 $\mu$ L                                       | 808 nm, 1 W cm <sup>-2</sup> , 3 min   | Tumor regression  | 116  |
| UCNP/GO incorporated into silk fibroin nanofibers-based hydrogel  | PTT      | 4T1 tumor-bearing mice        | p.t.                 | 100 $\mu$ L                                       | 808 nm, 1 W cm <sup>-2</sup> , 5 min   | Tumor regression  | 111  |
| Ag <sub>3</sub> Au <sub>2</sub> nanoparticles, E72 Peptide and chitosan hydrogel  | PTT      | CAL-27 tumor-bearing mice     | p.t.                 | 50 $\mu$ L  | 808 nm, 1 W cm <sup>-2</sup> , 3 min   | Tumor regression  | 117  |
| Guanosine and PDA functionalized Au nanoparticles hydrogel  | PTT      | Cal-27 tumor-bearing mice     | p.t.                 | 100 $\mu$ L (every 3 days for a total of 5 times) | 808 nm, 2 W cm <sup>-2</sup> , 5 min   | Tumor regression  | 118  |
| PDA nanoparticles incorporated into PVA <sup>h</sup> hydrogel   | PTT      | 4T1 tumor-bearing mice        | i.t.                 | 100 $\mu$ L                                       | 808 nm, 1.5 W cm <sup>-2</sup> , 10 min (every 2 days)                             | Tumor regression  | 108  |
| GO and nano-hydroxyapatite incorporated into PEG and carboxymethyl chitosan hydrogel  | PTT      | 4T1 tumor-bearing mice        | i.t.                 | 50 $\mu$ L  | 808 nm, 3 W cm <sup>-2</sup> , 10 min (days 1, 3, 5 and 7)                         | Tumor regression  | 119  |
| AINPs <sup>i</sup> incorporated into PLGA-PEG-PLGA <sup>j</sup> hydrogel  | PTT      | HCT-116 tumor-bearing mice    | i.t.                 | 60 $\mu$ L  | 1064 nm, 0.5 W cm <sup>-2</sup> , 15 min   | Tumor growth reduction  | 113  |
| D <sub>4</sub> EPTs <sup>k</sup> incorporated into alginate/Ca <sup>2+</sup> hydrogel   | PTT      | PC-9 tumor-bearing mice       | i.t.                 | 30 $\mu$ L  | 808 nm, 0.68 W cm <sup>-2</sup> , 5 min (every three days for a total of 10 times) | Tumor growth reduction  | 120  |
| CuS nanodots incorporated into Pluronic F127 hydrogel   | PTT      | 4T1 tumor-bearing mice        | p.t.                 | 500 $\mu$ L                                       | 808 nm, 1 W cm <sup>-2</sup> for 5 min   | Tumor growth reduction  | 105  |
| MnFe <sub>2</sub> O <sub>4</sub> /MoS <sub>2</sub> nanosheets incorporated into Chitosan-g-dihydrocaffeic acid and Pluronic F127-aldehyde micelles hydrogel | PTT      | A375 tumor-bearing mice       | i.t.                 | 50 $\mu$ L  | 808 nm, 1 W cm <sup>-2</sup> , 5 min (day 0 and day 1)                             | Tumor growth reduction  | 121  |
| Ti <sub>3</sub> C <sub>2</sub> nanosheets incorporated into PLA-PEG-PLA hydrogel  | PTT      | 4T1 tumor-bearing mice        | i.t.                 | 100 $\mu$ L                                       | 1064 nm, 1 W cm <sup>-2</sup> , 5 min  | Tumor growth reduction  | 122  |
| PB <sup>l</sup> nanoparticles incorporated into gellan gum hydrogel   | PTT      | 4T1 tumor-bearing mice        | i.t.                 | 100 $\mu$ L                                       | 808 nm, 1 W cm <sup>-2</sup> , 3 min   | Tumor growth reduction  | 123  |
| PDA-coated PEGylated Au nanorods, alginate-dopamine and chitosan/ $\beta$ -glycerophosphate hydrogel  | PTT      | HepG2 tumor-bearing mice      | p.t.                 | 200 $\mu$ L                                       | 808 nm, 1.5 W cm <sup>-2</sup> , 3 min (every 3 days for a total of 3 times)       | Tumor growth reduction  | 106  |
| BP <sup>m</sup> nanosheets incorporated into epichlorohydrin and Cellulose hydrogel   | PTT      | SMMC-7721 tumor-bearing mice  | i.t.                 | 100 $\mu$ L                                       | 808 nm, 1 W cm <sup>-2</sup> , 5 min   | Tumor growth reduction  | 124  |
| DEPTs <sup>n</sup> and dextran-aldehyde hydrogel  | PTT      | MDA-MB-231 tumor-bearing mice | i.t.                 | $\approx$ 30 $\mu$ L                              | 808 nm, 0.54 W cm <sup>-2</sup> , 5 min (every 2 days for a total of 4 times)      | Tumor growth reduction  | 125  |
| PB nanoparticles incorporated into gellan gum hydrogel  | PTT      | 4T1 tumor-bearing mice        | i.t.                 | 100 $\mu$ L                                       | 808 nm, 0.5 W cm <sup>-2</sup> , 5 min   | Tumor growth reduction  | 126  |

<sup>a</sup> Poly(*N*-isopropylacrylamide-*co*-dopamine methacrylamide). <sup>b</sup> Intratumoral. <sup>c</sup> Poly(lactic-*co*-glycolic) acid. <sup>d</sup> Peritumoral. <sup>e</sup> Upconversion lanthanide nanoparticles. <sup>f</sup> Salmon sperm DNA. <sup>g</sup> Subcutaneous. <sup>h</sup> Poly(vinyl alcohol). <sup>i</sup> Ancient ink nanoparticles. <sup>j</sup> Poly(*D,L*-lactic acid-*co*-glycolic acid)-*b*-poly(ethylene glycol)-*b*-poly(*D,L*-lactic acid-*co*-glycolic acid). <sup>k</sup> Pt nanoparticles loaded acetylated-poly(amidoamine) dendrimer. <sup>l</sup> Prussian blue. <sup>m</sup> Black phosphorus. <sup>n</sup> Pt nanoparticles loaded poly(amidoamine) dendrimer.





**Fig. 2** Schematic representation of therapeutic strategies based on injectable hydrogels incorporating nanomaterials aimed at cancer PTT and respective combinatorial-PTT approaches. (A–D) Main mechanism involved in injectable hydrogel PTT. (A) Inhibition of the DNA repair mechanisms induced by temperature increase. (B) ROS formation after the photothermally triggered tumor oxygenation. (C) Protein denaturation and mitochondria dysfunction caused by the photothermal heating. (D) Collapse of the cell membrane due to the local hyperthermia. (E–H) Key effects in injectable hydrogel photodynamic-PTT. (E) PDT-induced inflammatory response. (F) Improved tumor oxygenation (consequence of PTT) and production of ROS. Modified mitochondrial permeability prompted by ROS. (G) Affected DNA repair mechanism by the PDT-created ROS. (H) Hindered heat shock protein function by ROS. (I–L) Main events occurring in injectable hydrogel chemo-PTT. (I) Alteration of the hydrogel structure by photothermal heating and increased therapeutic agent release from the hydrogel. (J) Disruption of the extracellular matrix (as a consequence of the temperature increase), resulting in enhanced penetration of nanomaterials/drugs. (K) Photothermally triggered permeabilization of cell membrane leading to an enhanced internalization of the enrolled agents. (L) Affected DNA synthesis and repair mechanisms by chemotherapeutic action. (M–P) Main mechanism involved in injectable hydrogel immuno-PTT. (M) Macrophage polarization from a pro- to an anti-tumoral state due to the photothermally triggered hypoxia relief. Production of a pro-inflammatory response. (N) Photothermally induced release of tumor-associated antigens (TAAs) and damage-associated molecular patterns (DAMPs). (O) The released TAAs are processed by immature dendritic cells (DCs), leading to their maturation (aided by DAMPs) and subsequent priming and activation of cytotoxic T cells. (P) Enhanced DC maturation by the immunostimulants encapsulated in the hydrogels. CTLA-4, PD-L1 and PD-1 blockade by the immune checkpoint inhibitors encapsulated in the hydrogels. (Q–T) Key events taking place in injectable hydrogel radio-PTT. (Q) DNA breakage by ionizing radiation. (R) DNA breakage by the ROS produced after exposure to ionizing radiation. (S) Weakened DNA repair mechanisms (consequence of PTT) favor DNA breakage by ionizing radiation. (T) Photoinduced heat increases tumor oxygenation and improves radiotherapy efficacy.





Table 2 Injectable hydrogels for combinatorial PTT mediated by nanomaterials

| Hydrogel components   | Modality     | Tumor model                           | Administration route | Hydrogel volume | Laser parameters  | Therapeutic outcome of the combinatorial therapy | Therapeutic outcome of the single therapy | Ref. |
|---|--------------|---------------------------------------|----------------------|-----------------|---|--|---|------|
| Amido-modified carbon dots and aldehyde-modified cellulose nanocrystals hydrogel  | PTT          | B16F10 tumor-bearing mice             | i.t.                 | 50 $\mu$ L      | 660 nm, 0.22 W cm <sup>-2</sup> , 20 min                                    | Tumor eradication (4 out of 5)                   | —   | 135  |
| TMPPy <sup>d</sup> incorporated into collagen-Au nanoparticles hydrogel   | PDT          | MCF-7 tumor-bearing mice              | i.t.                 | —               | 635 nm, 0.17 W cm <sup>-2</sup> , 10 min (4 h and 12 h after the injection) | Tumor eradication (3 out of 4)                   | Tumor growth inhibition (PTT)             | 136  |
| ICG incorporated into PPG <sup>2</sup> -PEG and $\alpha$ -cyclodextrin hydrogel   | PDT          | 4T1 tumor-bearing mice                | i.t.                 | 100 $\mu$ L     | 808 nm, 0.14 W cm <sup>-2</sup> , 5 min (day 1, 3, 5 and 7)                 | Tumor eradication (2 out of 5)                   | Tumor growth reduction (PDT)              | 137  |
| TMPPy incorporated into AuNPs and collagen hydrogel   | PDT          | MCF-7 tumor-bearing mice              | i.t.                 | 50 $\mu$ L      | 635 nm, $\approx$ 0.170 mW cm <sup>-2</sup> , 10 min (day 0, 1, 2, 3 and 5) | Tumor eradication (2 out of 4)                   | Tumor growth reduction (PDT)              | 138  |
| BSA <sup>c</sup> -coated MoS <sub>2</sub> nanoflakes incorporated into oxidized sodium alginate and hydroxypropyl chitosan hydrogel | PDT          | 4T1 tumor-bearing mice                | i.t.                 | 50 $\mu$ L      | 808 nm, 3 W cm <sup>-2</sup> , 10 min (days 1, 3, 5, and 7)                 | Tumor growth reduction                           | —   | 139  |
| Ag <sub>2</sub> S quantum dots and PTX <sup>d</sup> incorporated into PC <sub>10</sub> A based hydrogel                             | PTT          | SKOV3 tumor-bearing mice              | i.t.                 | 100 $\mu$ L     | 808 nm, 2.5 W cm <sup>-2</sup> , 10 min                                     | Tumor eradication                                | Tumor growth reduction (PTT)              | 140  |
| DOX incorporated into Pd nanosheets and thiolated PEG (4-arm) hydrogel  | Chemotherapy | 4T1 tumor-bearing mice                | i.t.                 | —               | 808 nm, 0.6 W cm <sup>-2</sup> , 10 min                                     | Tumor eradication                                | Tumor growth reduction (chemo)            | 141  |
| DOX incorporated into polyacrylamide, phytic acid and PDA hydrogel  | Chemotherapy | SW620 tumor-bearing mice              | i.t.                 | —               | 808 nm, 0.75 W cm <sup>-2</sup> , 6 min                                     | Tumor eradication                                | Tumor growth reduction (PTT)              | 142  |
| PTX-loaded OSPC <sup>c</sup> -based micelles and PEGylated Au nanorods incorporated into poly F127-based hydrogel                   | PTT          | Hepatocellular carcinoma-bearing mice | i.t.                 | —               | 808 nm, 2 W cm <sup>-2</sup> , 10 min                                       | Tumor eradication                                | Tumor growth reduction (chemo)            | 143  |
| DOX loaded TPP <sup>f</sup> - and PHBA-functionalized AuMSN <sup>g</sup> and tyramine-HA hydrogel (HRP <sup>h</sup> as catalyzer)   | PTT          | MGC-803 tumor-bearing mice            | i.t.                 | 100 $\mu$ L     | 808 nm, 1 W cm <sup>-2</sup> , 10 min                                       | Tumor eradication                                | Tumor growth reduction (chemo)            | 144  |
| DOX and Au/Ag nanorods incorporated into alginate/Ca <sup>2+</sup> hydrogel   | PTT          | A549 tumor-bearing mice               | i.t.                 | 50 $\mu$ L      | 1064 nm, 1 W cm <sup>-2</sup> , 10 min (twice)                              | Tumor eradication (4 out of 5)                   | Tumor regression (chemo)                  | 145  |
| DOX loaded hollow Au nanoshells incorporated into PC <sub>10</sub> A based hydrogel   | PTT          | HepG2 tumor-bearing mice              | i.t.                 | 100 $\mu$ L     | 808 nm, 2 W cm <sup>-2</sup> , 9 min  | Tumor eradication (4 out of 6)                   | Tumor growth reduction (chemo)            | 146  |
| PEGylated <sup>i</sup> IDT-BTzTP <sup>j</sup> nanodots and DOX incorporated into agarose hydrogel                                   | PTT          | 4T1 tumor-bearing mice                | i.t.                 | 100 $\mu$ L     | 808 nm, 0.75 W cm <sup>-2</sup> , 10 min                                    | Tumor regression                                 | Tumor growth reduction (chemo)            | 147  |
| PB nanoparticles and DOX incorporated into PEI-NIPAM-nanosized cellulose, alginate and chitosan hydrogel                            | PTT          | MCF-7 tumor-bearing mice              | s.c.                 | 200 $\mu$ L     | 808 nm, 1.0 W cm <sup>-2</sup> , 30 min (every 2 days, a total of 3 times)  | Tumor regression                                 | Tumor growth reduction (chemo)            | 139  |
| DOX incorporated into Au nanobipyramids, Pt nanoclusters and 4 arm-PEG hydrogel   | PTT          | 4T1 tumor-bearing mice                | i.t.                 | —               | 808 nm, 0.5 W cm <sup>-2</sup> , 10 min                                     | Tumor regression                                 | Tumor growth reduction (PTT)              | 148  |
| Bi <sub>2</sub> S <sub>3</sub> nanodots and Sorafenib incorporated into gellan gum hydrogel   | PTT          | 4T1-Luc tumor-bearing mice            | i.t.                 | 100 $\mu$ L     | 808 nm, 1 W cm <sup>-2</sup> , 5 min  | Tumor regression                                 | Tumor growth reduction (chemo)            | 149  |



Table 2 (Contd.)

| Hydrogel components  | Modality     | Tumor model                   | Administration route | Hydrogel volume | Laser parameters  | Therapeutic outcome of the combinational therapy | Therapeutic outcome of the single therapy | Ref. |
|--|--------------|-------------------------------|----------------------|-----------------|---|--|---|------|
| Cisplatin incorporated into PEGylated PNPG <sup>5</sup> and $\alpha$ -cyclodextrin hydrogel  | PTT          | MDA-MB-231 tumor-bearing mice | i.t.                 | 100 $\mu$ L     | 1064 nm, 0.5 W cm <sup>-2</sup> , 5 min (every 2 days for a total of 4 times) | Tumor regression                                 | Tumor growth reduction (PTT)              | 150  |
| DOX incorporated into PAA <sup>1</sup> -PNIPAM-PAA/polypyrrole and hydrogel  | Chemotherapy | H22 tumor-bearing mice        | i.t.                 | 50 $\mu$ L      | 808 nm, 0.4 W cm <sup>-2</sup> , 5 min (at days 1, 2, 3, 4, 5, 8, and 10)     | Tumor regression                                 | Tumor growth reduction (chemo)            | 151  |
| Cisplatin/PDA-functionalized nano-hydroxyapatite, oxidized sodium alginate and chitosan hydrogel   | PTT          | 4T1 tumor-bearing mice        | i.t.                 | —               | 808 nm, 2 W cm <sup>-2</sup> , 2 min  | Tumor regression                                 | Tumor growth reduction (chemo)            | 152  |
| DOX and PEGylated MoS <sub>2</sub> /Bi <sub>2</sub> S <sub>3</sub> nanosheets incorporated into alginate/Ca <sup>2+</sup> hydrogel           | Chemotherapy | HT29 tumor-bearing mice       | i.t.                 | 50 $\mu$ L      | 808 nm, 0.8 W cm <sup>-2</sup> , 5 min  | Tumor regression                                 | Tumor growth reduction (PTT)              | 153  |
| DTX <sup>10</sup> loaded chitosan-GO incorporated into Poloxamer 407 and Poloxamer 188 hydrogel  | Chemotherapy | S180 tumor-bearing mice       | i.t.                 | —               | 808 nm, 2.5 W cm <sup>-2</sup> , 1 min (every day for a total of 12 days)     | Tumor regression                                 | Tumor growth reduction (chemo)            | 154  |
| DOX-loaded MnO <sub>2</sub> nanosheet and caffeic acid-chitosan hydrogel   | PTT          | A375 tumor-bearing mice       | i.t.                 | 50 $\mu$ L      | 808 nm, 1 W cm <sup>-2</sup> , 5 min (day 0 and day 1)                        | Tumor regression                                 | Tumor growth reduction (PTT)              | 75   |
| PDA nanoparticles and DOX incorporated into PNS <sup>6</sup> hydrogel  | Chemotherapy | H22 tumor-bearing mice        | i.t.                 | 100 $\mu$ L     | 808 nm, 1 W cm <sup>-2</sup> , 5 min (at days 1, 3, 5 and 7)                  | Tumor regression                                 | Tumor growth reduction (chemo)            | 155  |
| DOX and PDA nanoparticles incorporated into PNIPAM-co-sulfobetaine methacrylate and <i>N,N'</i> -methylenebisacrylamide hydrogel             | Chemotherapy | H22 tumor-bearing mice        | i.t.                 | 100 $\mu$ L     | 808 nm, 1.0 W cm <sup>-2</sup> , 5 min (days 1, 3, 5 and 7)                   | Tumor regression                                 | Tumor growth reduction (chemo)            | 155  |
| Oxaliplatin-cucurbit[7]uril supramolecular complex incorporated into chitosan-functionalized Au nanoparticles and OKGM <sup>9</sup> hydrogel | PTT          | HCT116 tumor-bearing mice     | i.t.                 | 100 $\mu$ L     | 808 nm, 2 W cm <sup>-2</sup> , 10 min (at days 0, 1, 3, 4)                    | Tumor growth inhibition                          | Tumor growth reduction (chemo)            | 156  |
| Curcumin loaded PLGA microspheres and IR820 incorporated into methylcellulose hydrogel   | Chemotherapy | K7M2 wt tumor-bearing mice    | p.t.                 | 100 $\mu$ L     | 808 nm 2.5 W cm <sup>-2</sup> , 5 min   | Tumor growth inhibition                          | Tumor growth reduction (chemo)            | 110  |
| Berberin loaded glycyrrhetic acid-PEG-functionalized GO incorporated into Poloxamer 188 and Poloxamer 407 hydrogel                           | PTT          | S180 tumor-bearing mice       | i.t.                 | —               | 808 nm, 2.5 W cm <sup>-2</sup> , 2 min  | Tumor growth reduction                           | Tumor growth reduction (chemo)            | 107  |
| ICG incorporated into sodium selenite and HA-dopamine hydrogel   | Chemotherapy | MDA-MB-231 tumor-bearing mice | i.t.                 | 100 $\mu$ L     | 808 nm, 0.3 W cm <sup>-2</sup> , 10 min (day 1, 4, 10, and 14)                | Tumor growth reduction                           | Tumor growth reduction (PTT)              | 157  |
| BP nanosheets and Gemcitabine incorporated into Pluronic F127 hydrogel   | PTT          | 4T1 tumor-bearing mice        | i.t.                 | 200 $\mu$ L     | 808 nm, 2 W cm <sup>-2</sup> , 5 min  | Tumor growth reduction                           | Tumor growth reduction (chemo)            | 158  |
| PEGylated MoS <sub>2</sub> /Bi <sub>2</sub> S <sub>3</sub> nanosheets and DOX incorporated into agar hydrogel                                | Chemotherapy | HT29 tumor-bearing mice       | i.t.                 | 50 $\mu$ L      | 808 nm, 1 W cm <sup>-2</sup> , 5 min  | Tumor growth reduction                           | Tumor growth reduction (PTT)              | 65   |
| PEGylated MoS <sub>2</sub> /Bi <sub>2</sub> S <sub>3</sub> nanosheets and DOX incorporated into chitosan/ $\beta$ -glycerophosphate hydrogel | Chemotherapy | HT29 tumor-bearing mice       | i.t.                 | 50 $\mu$ L      | 808 nm, 1 W cm <sup>-2</sup> , 5 min (5 min after injection)                  | Tumor growth reduction                           | Tumor growth reduction (chemo)            | 85   |





Table 2 (Contd.)

| Hydrogel components  | Modality      | Tumor model                         | Administration route | Hydrogel volume | Laser parameters   | Therapeutic outcome of the combinational therapy | Therapeutic outcome of the single therapy  | Ref. |
|--|---------------|-------------------------------------|----------------------|-----------------|--|--|--|------|
| BP nanosheets and PTX incorporated into OSA <sup>2</sup> and aminated-HA hydrogel  | PTT           | SGC7901 tumor-bearing mice          | i.t.                 | 100 µL          | 808 nm, 1.5 W cm <sup>-2</sup> , 5 min   | Tumor growth reduction                           | Tumor growth reduction (PTT)<br>Tumor growth reduction (chemo)   | 159  |
| PDS <sup>4</sup> , Ascorbic Acid, DOX and PDPBPT loaded Pluronic F127 nanoparticles incorporated into benzoxaborole modified HA and Poly-Fru <sup>7</sup> hydrogel | PTT           | 4T1 tumor-bearing mice              | p.t.                 | 50 µL           | 660 nm, 0.5 W cm <sup>-2</sup> , 20 min irradiation (day 1), 915 nm, 0.5 W cm <sup>-2</sup> , 10 min (day 3) | Tumor growth reduction                           | Tumor growth reduction (PTT)<br>Tumor growth reduction (chemo)   | 160  |
| SN38 <sup>8</sup> loaded PDA nanoparticles and thiolated PEG (4-arm) hydrogel  | PTT           | PC-9 tumor-bearing mice             | i.t.                 | 30 µL           | 808 nm, 0.58 W cm <sup>-2</sup> , 5 min, (every 2 days for a total of 4 times)                               | Tumor growth reduction                           | Tumor growth reduction (PTT)<br>Tumor growth reduction (chemo)   | 161  |
| mPEG <sup>9</sup> -PCT <sup>10</sup> functionalized Au nanorods/α-CD and PTX-loaded mPEG-PCT nanoparticles/α-cyclodextrin hydrogel                                 | PTT           | 4T1 tumor-bearing mice              | s.c.                 | —               | 808 nm, 1.5 W cm <sup>-2</sup> , 5 min (every 2 days for a total of 4 times)                                 | Tumor growth reduction                           | Tumor growth reduction (PTT)<br>Tumor growth reduction (chemo)   | 162  |
| PEGylated Au nanorods and TPGS <sup>11</sup> /PTX nanocrystals incorporated into Pluronic F127 and Pluronic F68 hydrogel   | PTT           | SW620 AD300 tumor-bearing mice      | p.t.                 | 200 µL          | 808 nm, 2 W cm <sup>-2</sup> , 3 min (day 2 and 8)   | Tumor growth reduction                           | Tumor growth reduction (PTT)<br>Tumor growth reduction (chemo)   | 163  |
| PDA nanoparticles and DOX incorporated into PEI and SP(DMAEMA-co-HEMAA) <sup>12</sup> hydrogel   | PTT           | 4T1 tumor-bearing mice              | i.t.                 | 50 µL           | 808 nm, 1 W cm <sup>-2</sup> , 10 min (every 2 days for a total of 4 times)                                  | Tumor growth reduction                           | Tumor growth reduction (PTT)<br>Tumor growth reduction (chemo)   | 164  |
| PEGylated Au nanorods, NIPAm <sup>13</sup> , AD-DOX <sup>14</sup> loaded MPCD <sup>15</sup> hydrogel (APS <sup>16</sup> and ascorbic acid as initiator)            | PTT           | S <sub>180</sub> Tumor-bearing mice | i.t.                 | 200 µL          | 785 nm, 1 W cm <sup>-2</sup> , 10 min (at days 2, 4, and 6)  | Tumor growth reduction                           | Tumor growth reduction (chemo)<br>Tumor growth reduction (PTT)<br>Tumor growth reduction (chemo)   | 165  |
| DOX-loaded mesoporous PDA nanoparticles incorporated into curcumin-cyclodextrin, oxidized HA and hydroxypropyl chitosan hydrogel                                   | PTT           | Hepa 1-6 tumor-bearing mice         | i.t.                 | 100 µL          | 808 nm, 1 W cm <sup>-2</sup> , 5 min (day 1 and 3)   | Tumor growth reduction                           | Tumor growth reduction (PTT)<br>Tumor growth reduction (chemo)   | 166  |
| DOX loaded Zeolitic imidazolate frameworks and CuS nanoparticles incorporated into methylcellulose and carboxymethyl chitosan hydrogel                             | PTT           | 4T1 tumor-bearing mice              | i.t.                 | 50 µL           | 808 nm, 1 W cm <sup>-2</sup> , 5 min (days 1, 3, 5, and 7)   | Tumor growth reduction                           | Tumor growth reduction (chemo)<br>Tumor growth reduction (chemo)   | 167  |
| Ag nanoparticles-doped SnS <sub>2</sub> nanoflowers and DOX incorporated into agarose hydrogel   | PTT           | 4T1 tumor-bearing mice              | i.t.                 | 100 µL          | 808 nm, 1.2 W cm <sup>-2</sup> , 10 min  | Tumor growth reduction                           | Tumor growth reduction (PTT)<br>Tumor growth reduction (chemo)   | 168  |
| BSA-coated MnO <sub>2</sub> nanoparticles and R848 incorporated into HA and Pluronic F127 hydrogel   | PTT           | 4T1 tumor-bearing mice              | i.t.                 | 50 µL           | 808 nm, 2 W cm <sup>-2</sup> , 10 min  | Primary Tumor growth inhibition                  | Primary tumor growth reduction (chemo)<br>Primary tumor growth reduction (PTT)<br>Secondary tumor growth reduction (PTT)<br>Secondary tumor growth reduction (immuno)<br>Secondary tumor growth reduction (immuno) | 169  |
|  | Immunotherapy |                                     |                      |                 |  | Secondary tumor growth reduction                 |  |      |

Table 2 (Contd.)

| Hydrogel components   | Modality      | Tumor model                  | Administration route | Hydrogel volume | Laser parameters   | Therapeutic outcome of the combinational therapy                                  | Therapeutic outcome of the single therapy  | Ref. |
|---|---------------|------------------------------|----------------------|-----------------|--|---|--|------|
| ICG and R837 incorporated into chitosan, $\beta$ -glycerophosphate, and HA hydrogel   | PTT           | 4T1 tumor-bearing mice       | i.p.                 | 100 $\mu$ L     | 808 nm, 1 W cm <sup>-2</sup> , 10 min (day 3 and day 7)  | Primary tumor eradication (8 out of 10)   | Primary tumor eradication (4 out of 8) (PTT)<br>No effect on the secondary tumor growth (PTT)<br>Primary tumor growth reduction (immuno)   | 109  |
| Methylene blue and R837 incorporated into collagen and alginate hydrogel  | PTT           | 4T1 tumor-bearing mice       | i.t.                 | 50 $\mu$ L      | 660 nm, 0.5 W cm <sup>-2</sup> , 10 min  | Primary tumor eradication<br>Secondary tumor growth reduction<br>Tumor regression | —  | 170  |
| Thymopentin and biliverdin incorporated into thiolated PLL <sup>66</sup> and Fmoc-FR <sup>66</sup> hydrogel                                 | PTT           | Pan02-luc tumor-bearing mice | i.t.                 | 100 $\mu$ L     | 730 nm, 0.5 W cm <sup>-2</sup> , 10 min  | —   | Tumor growth reduction (PTT)<br>Tumor growth reduction (immuno)  | 171  |
| ICG, R848 and CpG ODNs nanoparticles incorporated into PDLLA-PEG-PDLLA <sup>66</sup> hydrogel   | PTT           | 4T1-Luc tumor-bearing mice   | p.t.                 | —               | 808 nm, 1.5 W cm <sup>-2</sup> , 5 min (day 1, 3 and 5)  | Recurrent tumor growth reduction  | Recurrent tumor growth reduction (PTT)<br>Recurrent tumor growth reduction (immuno)  | 172  |
| PB nanoparticles incorporated into Agarose hydrogel   | PTT           | 4T1 tumor-bearing mice       | i.t.                 | —               | 808 nm, 1 W cm <sup>-2</sup> , 5 min;  | Tumor regression  | Recurrent tumor growth reduction (immuno)<br>Tumor growth reduction (PTT)  | 173  |
| DOX loaded MoS <sub>2</sub> nanosheets incorporated into PC <sub>10</sub> A based hydrogel  | PTT<br>PDT    | 4T1 tumor-bearing mice       | i.t.                 | 100 $\mu$ L     | 2 Gy, 5 min (6 h after NIR irradiation)<br>808 nm, 1.5 W cm <sup>-2</sup> , 10 min                                       | Tumor eradication (4 out of 5)  | Tumor growth reduction (radio)<br>Tumor growth reduction (PTT + PDT)   | 174  |
| TiO <sub>2</sub> /MWCNT <sup>66</sup> and DOX incorporated into PEGDA <sup>6f</sup> hydrogel (TiO <sub>2</sub> /MWCNT and NIR as initiator) | PTT<br>PDT    | S180 tumor-bearing mice      | i.t.                 | 100 $\mu$ L     | 808 nm, 1 W cm <sup>-2</sup> , 2 min (day 1, for hydrogel formation)   | Tumor regression  | Tumor growth reduction (chemo)<br>Tumor growth reduction (PDT + PTT)   | 175  |
| DOX-loaded mesoporous silica nanoparticles and IR820 incorporated into methylcellulose hydrogel   | PTT<br>PDT    | Cal27 tumor-bearing mice     | p.t.                 | 100 $\mu$ L     | 808 nm, 1.5 W cm <sup>-2</sup> , 3 min (once every 2 days)<br>808 nm, 2.0 W cm <sup>-2</sup> , 5 min (at day 1, 3 and 6) | Tumor regression  | Tumor growth reduction (chemo)<br>Tumor growth reduction (PTT)<br>Tumor regression (chemo)   | 176  |
| Ag <sub>2</sub> S quantum dots, DOX and bestatin incorporated into PC <sub>10</sub> ARGD based hydrogel                                     | PTT           | 4T1 tumor-bearing mice       | i.t.                 | 50 $\mu$ L      | 808 nm, 2 W cm <sup>-2</sup> , 7 min   | Tumor growth reduction  | Tumor growth reduction (PTT + chemo)<br>Tumor growth reduction (PTT + immuno)<br>Tumor growth reduction (PTT)<br>Tumor growth reduction (immuno)<br>Tumor growth reduction (chemo) | 177  |
|   | Chemotherapy  |                              |                      |                 |  |   |  |      |
|   | Immunotherapy |                              |                      |                 |  |   |  |      |





Table 2 (Contd.)

| Hydrogel components   | Modality     | Tumor model              | Administration route | Hydrogel volume | Laser parameters   | Therapeutic outcome of the combinatorial therapy | Therapeutic outcome of the single therapy | Ref. |
|---|--------------|--------------------------|----------------------|-----------------|--|--|---|------|
| Au nanoparticles aggregates and DOX incorporated into <sup>131</sup> I-labelled PEG-P(Tyrosine) <sub>8</sub> hydrogel | PTT          | MCF-7 tumor-bearing mice | p.t.                 | 100 µL          | 808 nm, 2 W cm <sup>-2</sup> , 10 min (at day 1, 3, and 5) | Tumor growth reduction                           | Tumor growth reduction (chemo + radio)    | 178  |
|   | Chemotherapy |                          |                      |                 |  |  | Tumor growth reduction (chemo + PTT)      |      |
|   | Radiotherapy |                          |                      |                 |  |  | Tumor growth reduction (radio + PTT)      |      |

<sup>a</sup> Meso-tetra (N-methyl-4-pyridyl) porphine tetrachloride. <sup>b</sup> Poly(N-phenylglycine). <sup>c</sup> Bovine serum albumin. <sup>d</sup> Paclitaxel. <sup>e</sup> N-Octyl-N, O-succinyl-O-phosphoryl chitosan. <sup>f</sup> Triphenylphosphine. <sup>g</sup> Au-core mesoporous silica nanoparticles. <sup>h</sup> Horseradish peroxidase. <sup>i</sup> Polystyrene-g-PEG. <sup>j</sup> Poly[(4,4,9,9-tetraakis(4-hexylphenyl)-4,9-dihydro-sindaceno [1,2-b:5,6-b'] dithiophene-2,7-diyl)-co-[6-(2-ethylhexyl)-1,2,5]thiadiazolo[3,4-f]benzotriazole-4,8-divyl]. <sup>k</sup> Poly(N-phenylglycine). <sup>l</sup> Poly(acrylic acid-*b*-N-isopropylamide-*b*-acrylic acid. <sup>m</sup> Docetaxel. <sup>n</sup> PNIPAM-poly(sulfobetaine methacrylate) crosslinked with N,N-methylenebisacrylamide. <sup>o</sup> Oxidized-konjac glucomanan. <sup>p</sup> Oxidized sodium alginate. <sup>q</sup> Perylene diimide zwitterionic polymer. <sup>r</sup> Fructose-based glycopolymer. <sup>s</sup> 7-Ethyl-10-hydroxycamptothecin. <sup>t</sup> Methoxy PEG. <sup>u</sup> Poly( $\epsilon$ -caprolactone-co-1,4,8-trioxol[4,6]spiro-9-undecaneone). <sup>v</sup>  $\alpha$ -Tocopherol PEG1000 succinate. <sup>w</sup> Star-shaped poly(2-(dimethylamino)ethyl methacrylate-co-2-hydroxyethyl methacrylate) modified with tertbutyl acetoacetate (t-BAA). <sup>x</sup> N-Isopropylacrylamide. <sup>y</sup> Adamantane-modified DOX. <sup>z</sup> Methacrylated  $\beta$ -cyclodextrin-based macromer. <sup>aa</sup> Ammonium persulfate. <sup>ab</sup> Poly-L-lysine. <sup>ac</sup> N-Florenylmethoxycarbonyl diphenylalanine. <sup>ad</sup> Poly(D,L-lactide)-block-poly(ethylene glycol)-block-poly(D,L-lactide). <sup>ae</sup> Multi-walled carbon nanotube. <sup>af</sup> PEG diacrylate.

flow in the irradiated area, improving tumor oxygenation and hence boosting the production of ROS by the photosensitizers.<sup>179,180</sup> On the other hand, the ROS produced during PDT can hinder the function of heat shock proteins which are overexpressed by cancer cells and protect them against the heat-induced damage generated in PTT.<sup>13,181</sup> In an ideal situation, both the photothermal nano-agent and the photosensitizer would be responsive to the same wavelength of NIR light, enabling a straightforward single-irradiation treatment.<sup>12,13</sup> When these agents have very distinct optical properties (*i.e.*, the wavelengths of their maximum absorption are distinct), sequential irradiation with lasers emitting light at different wavelengths is required.<sup>12,13,182</sup>

Sun *et al.* prepared an injectable hydrogel by mixing collagen and AuCl<sub>4</sub><sup>-</sup> that achieved gelation through electrostatic interactions.<sup>136</sup> In this process, Au nanoparticles (AuNPs) are simultaneously formed in the hydrogel's matrix. In addition, the water-soluble photosensitizer meso-tetra(N-methyl-4-pyridyl) porphine tetrachloride (TMPyP) was also included in the hydrogel matrix.<sup>136</sup> By using 635 nm laser light (0.17 W cm<sup>-2</sup>, 10 min; at 4 h and 12 h after the injection), the intratumorally injected hydrogel incorporating AuNPs and TMPyP (combinatorial photodynamic-PTT) could eradicate the breast tumors in 3 out of 4 mice (Fig. 3). On the other hand, the stand-alone PTT could only promote the elimination of the breast tumor in 1 mouse, while the stand-alone PDT only reduced the tumor's growth.<sup>136</sup>

#### 4.2. Injectable hydrogels for cancer chemo-PTT

The use of injectable hydrogels for the co-delivery of nano-photothermal agents and chemotherapeutics has also been extensively researched (Table 2). Depending on the water solubility of the chemotherapeutic agents, these can either be incorporated into the hydrogel's hydrophilic network or loaded in the hydrophobic regions of the photothermal nano-agents.<sup>56</sup> Another strategy for loading hydrophobic chemotherapeutics in injectable hydrogels relies on the introduction of hydrophobic moieties (*e.g.*, amphiphilic polymers<sup>183</sup>) or molecules capable of forming complexes (*e.g.*, cyclodextrins<sup>183</sup>) in the hydrogel matrix.<sup>56</sup>

The local delivery of chemotherapeutic drugs using injectable hydrogels is more controlled/sustained and shields healthy tissues from possible side effects.<sup>53,72</sup> Furthermore, the photothermal heating of nanomaterials can (i) disrupt the extracellular matrix and cell membrane, boosting the penetration and internalization of chemotherapeutic drugs, and (ii) interfere with the structural network of some hydrogels (thermo-responsive), stimulating the chemotherapeutics' release (Fig. 2I-L).<sup>10,184</sup>

Zhou and co-workers prepared AuNPs coated with a mesoporous silica shell that were loaded with DOX and functionalized with triphenylphosphine.<sup>144</sup> Upon injection, the phenolic groups of this nanostructure could react covalently with tyrosine-HA (reaction catalyzed by horseradish peroxidase), creating an *in situ*-forming hydrogel.<sup>144</sup> The release of DOX from this hydrogel was responsive to hyaluronidase-mediated degradation and to NIR light-induced photothermal heating. When



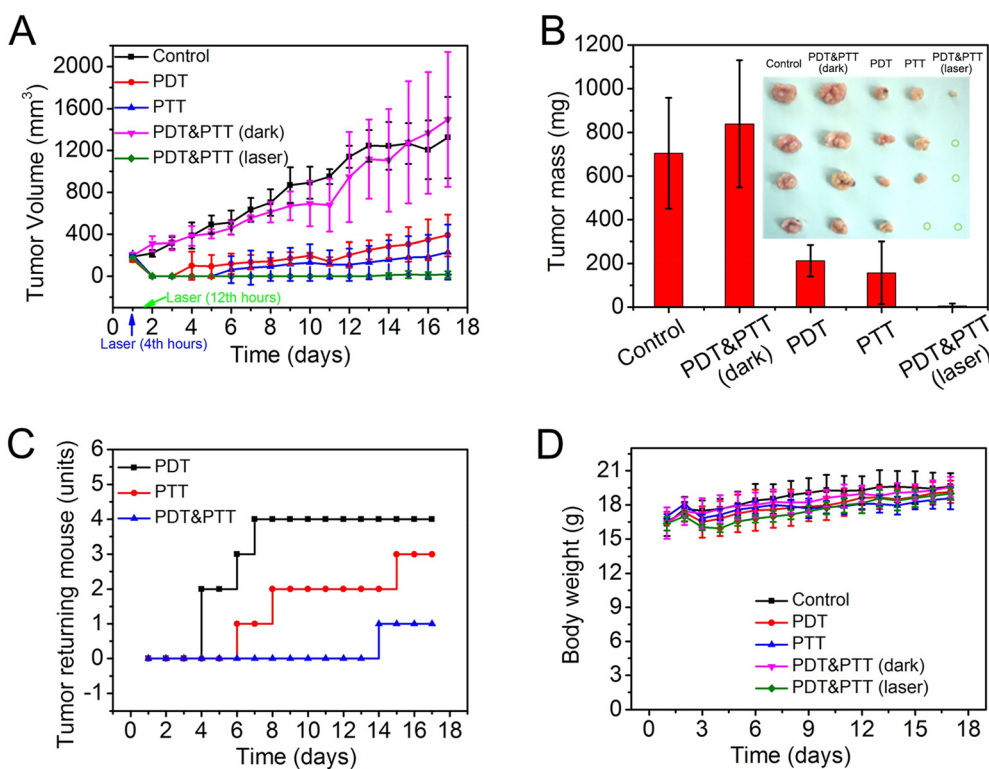


**Fig. 3** *In vivo* combinatorial PTT–PDT mediated by collagen-based injectable hydrogels incorporating AuNPs and TMPyP. Tumor volume (A), tumor mass (B), tumor recurrence (C) and body weight (D) after the various treatments. Control: collagen solution and laser irradiation (635 nm, 0.17 W cm<sup>-2</sup>, 10 min at 4 h and 12 h after injection); PDT: TMPyP solution and laser irradiation; PTT: collagen and AUNPs hydrogel with laser irradiation; PDT&PTT (dark): collagen and AUNPs hydrogel incorporating TMPyP; PDT&PTT (laser): collagen and AUNPs hydrogel incorporating TMPyP with laser irradiation. Reprinted with permission from ref. 136. Copyright 2016, Elsevier B.V.

tested *in vivo*, the chemo-PTT mediated by this hydrogel prompted tumor eradication, while the stand-alone therapies (hydrogel PTT or hydrogel chemotherapy) only induced tumor regression (Fig. 4).<sup>144</sup>

In another work, Jiang *et al.* developed an injectable hydrogel based on the chemical crosslinking occurring between palladium nanosheets (PTT agent) and the thiol pendant groups of branched 4-arm PEG, that also incorporated DOX.<sup>141</sup> This hydrogel mediated a sustained delivery of DOX, the amount of released drug being augmented upon NIR laser irradiation. When tested *in vivo*, the DOX-loaded palladium nanosheets-PEG hydrogel in combination with NIR light (808 nm, 0.6 W cm<sup>-2</sup>, 10 min) induced breast tumor eradication. In contrast, the stand-alone PTT (palladium nanosheets-PEG hydrogel plus NIR light) could reduce tumors' growth, while the stand-alone chemotherapy (DOX-loaded palladium nanosheets-PEG hydrogel) had a weak therapeutic outcome, being very similar to the control.<sup>141</sup>

### 4.3. Injectable hydrogels for cancer immuno-PTT

In general, therapeutic approaches based on the use of injectable hydrogels incorporating nanomaterials aimed at cancer PTT are not effective towards metastases nor prevent tumor's recurrence.<sup>185</sup> However, the photothermal heating triggers some events which, aided by immunotherapeutic agents (*e.g.*,

immunostimulants, immune checkpoint inhibitors), can lead to the establishment of anti-metastatic cytotoxic T-cell responses and the creation of immune memory.<sup>186–188</sup>

In fact, the local photothermal heating *per se* can (i) induce the release of tumor-associated antigens (TAA) and damage-associated molecular patterns (DAMPs) from cancer cells, (ii) enhance the blood flow into the tumor zone, relieving tumor hypoxia and thus driving macrophages' polarization from a pro to an anti-tumoral state, and (iii) generate a pro-inflammatory response.<sup>187,189–191</sup> Subsequently, the released TAA can be processed by antigen-presenting cells (*e.g.*, dendritic cells), paving the way for the priming and activation of cytotoxic T cells.<sup>192</sup> The TAA-primed cytotoxic T cells can then potentially mediate the elimination of local and metastasized tumors. In this process, immune memory may also be established, being crucial for the prevention of a tumor's recurrence.<sup>193</sup> To further boost these processes, the injectable hydrogels can be loaded with (i) immunostimulants (*e.g.*, toll-like receptors agonists) to enhance dendritic cell maturation, and (ii) immune checkpoint inhibitors (*e.g.*, CTLA-4 and PD-1/PD-L1 blockers, IDO1 inhibitors) to abolish the immunosuppressive interactions occurring in the tumor microenvironment (Fig. 2M–P).<sup>194</sup>

In a recent study, Revuri *et al.* developed an injectable hydrogel using Pluronic F127 and HA that incorporated bovine



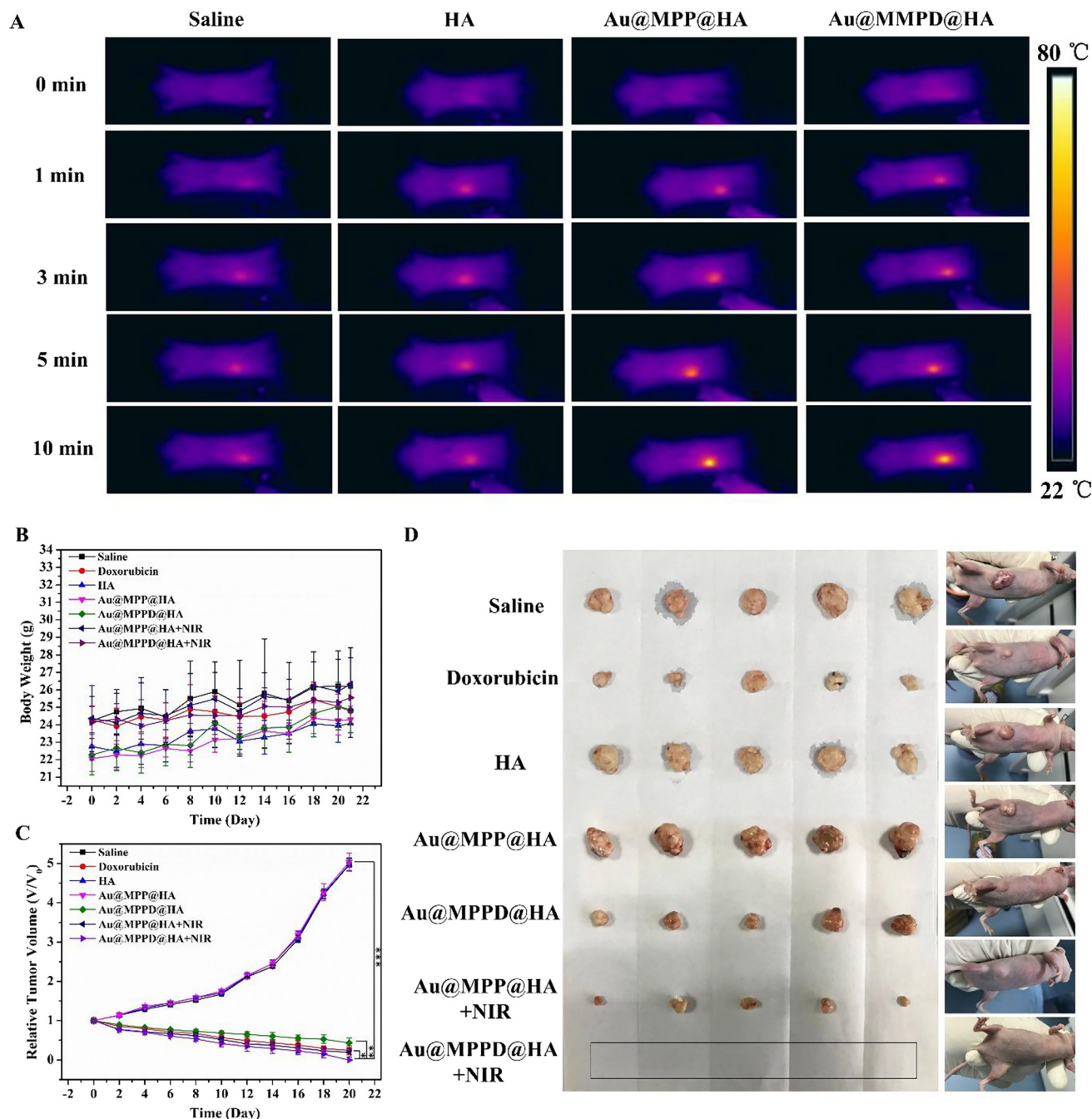


**Fig. 4** *In vivo* combinatorial chemo-PTT mediated by an injectable hydrogel based on tyrosine-HA and DOX loaded TPP-AuMSN. Thermographic images of mice after intratumoral administration of the formulations and exposure to NIR irradiation (808 nm, 1 W cm<sup>-2</sup>) (A). Body weight of the mice after each treatment (B). Relative tumor volume (C) and representative images of the tumors (D) after the different treatments. Au@MPP@HA: tyrosine-HA and TPP-AuMSN hydrogel; Au@MPPD@HA: tyrosine-HA and DOX-loaded TPP-AuMSN hydrogel; Au@MPP@HA + NIR tyrosine-HA and TPP-AuMSN hydrogel with NIR irradiation (808 nm, 1 W cm<sup>-2</sup>, 10 min); Au@MPPD@HA + NIR: tyrosine-HA and DOX-loaded TPP-AuMSN hydrogel with NIR irradiation. Reprinted with permission from ref. 144. Copyright 2020, American Chemical Society.

serum albumin modified-MnO<sub>2</sub> nanoparticles (BSA-MnO<sub>2</sub> nanoparticles) and resiquimod as photothermal and immunostimulating agents, respectively.<sup>169</sup> The assembly of this injectable hydrogel was based on the thermo-responsive behavior of Pluronic F127, which upon heating to body temperature underwent a sol-gel transition (HA was used to improve the

hydrogel's mechanical strength).<sup>169</sup> This formulation was then injected into primary tumors in mice, followed by NIR irradiation (808 nm, 2 W cm<sup>-2</sup>, 10 min), while the secondary tumors were not directly treated (Fig. 5). The immuno-PTT mediated by this injectable hydrogel could inhibit the growth of the primary tumor and reduce the growth of the secondary



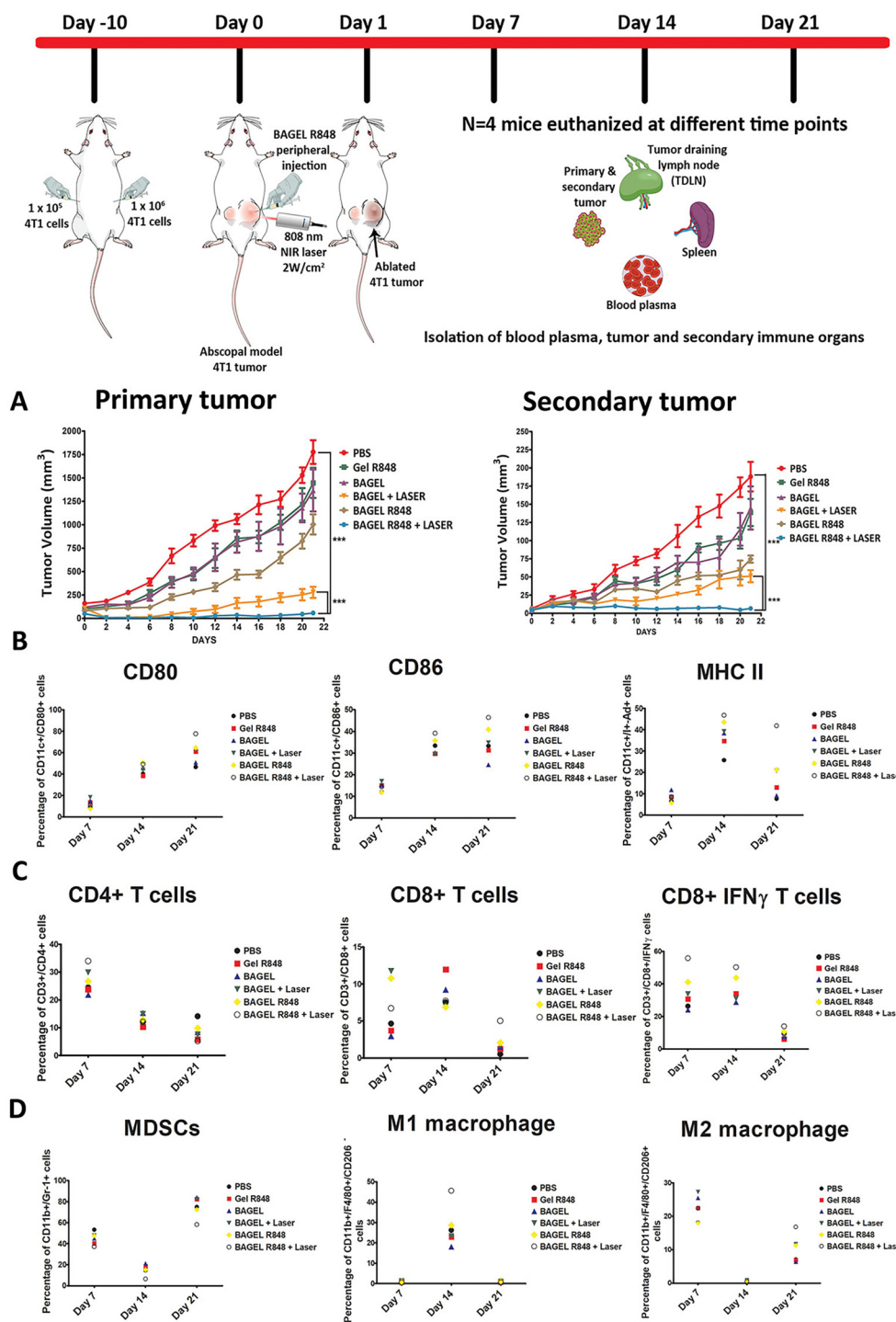


**Fig. 5** *In vivo* immuno-PTT mediated by an injectable hydrogel of HA-Pluronic F127 incorporating BSA-MnO<sub>2</sub> nanoparticles and resiquimod. Volume of the primary and secondary tumors (A). Percentage of CD80<sup>+</sup>, CD86<sup>+</sup> and MHCII<sup>+</sup> dendritic cells (B) and CD4<sup>+</sup>, CD8<sup>+</sup> and CD8<sup>+</sup>IFN $\gamma$  T cells (C). Gel R848: HA-Pluronic F127 hydrogel incorporating resiquimod; BAGEL: HA-Pluronic F127 hydrogel incorporating BSA-MnO<sub>2</sub> nanoparticles; BAGEL + LASER: HA-Pluronic F127 hydrogel incorporating BSA-MnO<sub>2</sub> nanoparticles with NIR irradiation (808 nm, 2 W cm<sup>-2</sup>, 10 min); BAGEL R848: HA-Pluronic F127 hydrogel incorporating BSA-MnO<sub>2</sub> nanoparticles and resiquimod; BAGEL R848 + LASER: HA-Pluronic F127 hydrogel incorporating BSA-MnO<sub>2</sub> nanoparticles and resiquimod with NIR irradiation. Reprinted with permission from ref. 169. Copyright 2021, Wiley-VCH GmbH.

tumor. Such effects were correlated with the ability of this treatment to prompt higher levels of matured dendritic cells and activated cytotoxic T cells at the secondary tumor sites.<sup>169</sup>

In another work, Zhang *et al.* produced an injectable hydrogel using *N*-fluorenylmethoxycarbonyl diphenylalanine and poly-L-lysine grafted with thiol-groups, that incorporated bili-





verdin (photothermal agent) and thymopentin (immunomodulatory peptide).<sup>171</sup> This hydrogel system presented a shear-thinning/self-healing behavior, being assembled through electrostatic and hydrophobic interactions,  $\pi$ - $\pi$  stacking and disulfide bonds. *In vivo*, the immuno-PTT mediated by this injectable hydrogel led to tumor regression, while the stand-alone therapies (hydrogel PTT or hydrogel immunotherapy) only prompted a reduction of the tumor's growth. The hypoxia relief, improved dendritic cell maturation, and enhanced T-cell recruitment mediated by the combinatorial treatment contributed to this therapeutic outcome.<sup>171</sup>

#### 4.4. Injectable hydrogels for cancer radio-PTT

Injectable hydrogels aimed at cancer PTT can also be combined with high-frequency radiation (*e.g.*, X-rays, gamma rays) with the intent to achieve a greater therapeutic outcome.<sup>13</sup> Such radio-photothermic application can also be performed by incorporating photothermal nano-agents and radionuclides (*e.g.*, <sup>131</sup>I) into the injectable hydrogels.<sup>195</sup> In this process, radiosensitizers (*e.g.*, SmacN7) may also be included to further boost the therapeutic outcome.<sup>178,195</sup>

On one hand, the delivery of radionuclides/radiosensitizers using injectable hydrogels into the tumor tissue can contribute to protecting healthy cells from the ionizing

radiation.<sup>196,197</sup> The ability of the produced photoinduced heat to improve tumor oxygenation also plays an important role in improving the therapeutic outcome (radiotherapy displays lower efficacy in hypoxic environments).<sup>13,198</sup> Moreover, such temperature increase can also weaken the DNA repair mechanism, being crucial to prevent the repair of the DNA double-strand breaks caused by radiotherapy.<sup>100</sup> On the other hand, the higher penetration depth of radiotherapeutic approaches can counterbalance the limitation of PTT in treating deep-seated tumors (NIR light has limited penetration depth) (Fig. 2Q–T).<sup>199</sup>

Wang and co-workers developed an injectable thermo-responsive hydrogel composed of agarose incorporating Prussian blue nanoparticles, which was combined with NIR and high-frequency radiation, for breast cancer radio-PTT.<sup>173</sup> Besides acting as the photothermal nano-agent, the Prussian blue nanoparticles also decomposed H<sub>2</sub>O<sub>2</sub> to produce O<sub>2</sub>, counteracting tumor hypoxia and acting as a radiosensitizer.<sup>173</sup> After administration of this formulation, the tumor area was irradiated with NIR light (808 nm, 1 W cm<sup>-2</sup>, 5 min) and high-energy radiation (2 Gy, 5 min, at 6 h post-PTT). This treatment resulted in tumor regression. In contrast, the application of stand-alone therapies only induced a reduction in tumor growth (Fig. 6).<sup>173</sup>

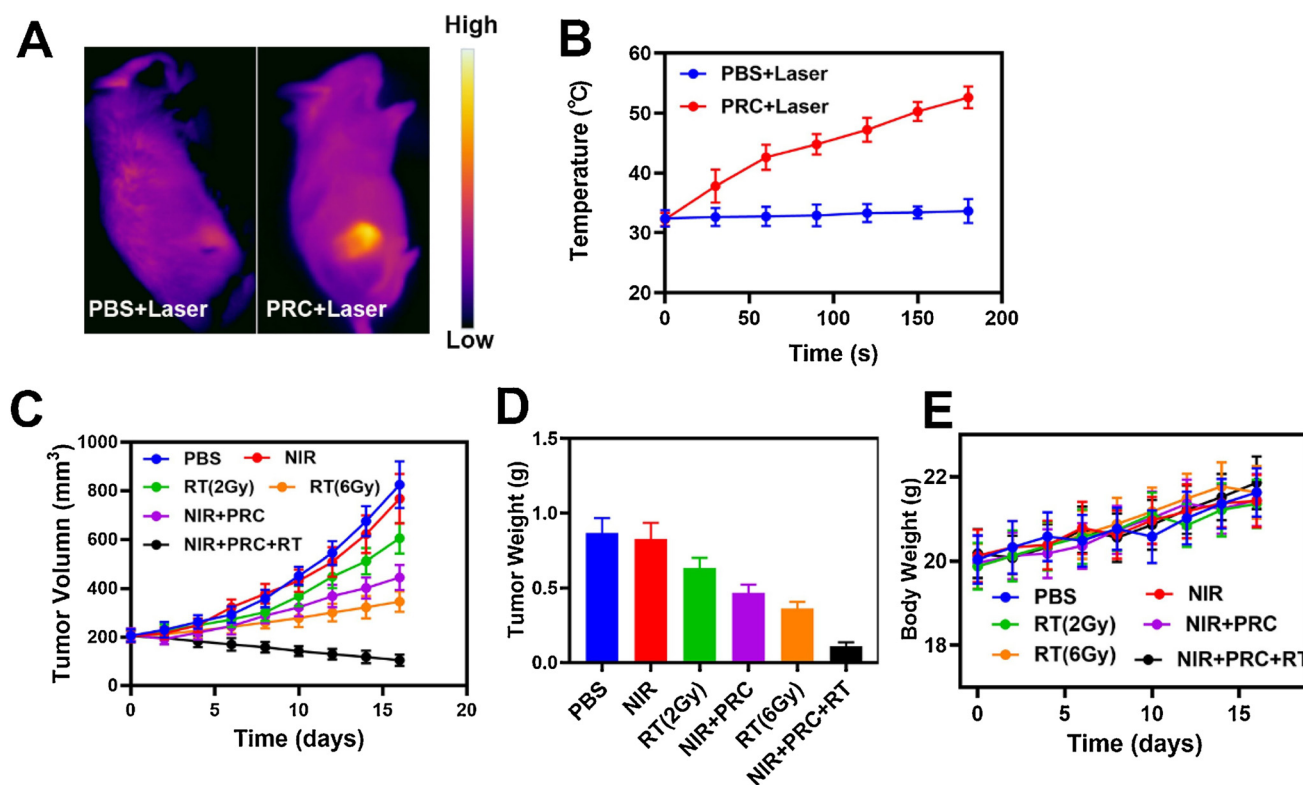


**Fig. 6** *In vivo* radio-PTT mediated by an agarose-based injectable hydrogel incorporating Prussian blue nanoparticles. Thermal images of mice (A) and temperature of the tumor zone (B) after exposure to phosphate-buffered saline or agarose hydrogel incorporating Prussian blue nanoparticles and NIR light (808 nm, 1 W cm<sup>-2</sup>, 5 min). Tumor volume (C), tumor weight (E) and body weight (D) of mice after the different treatments. NIR: NIR light (808 nm, 1 W cm<sup>-2</sup>, 5 min); RT (2 Gy): high-energy radiation (2 Gy, 5 min); RT (6 Gy): high-energy radiation (6 Gy, 5 min); NIR + PRC: Prussian blue NPs-agarose hydrogel and NIR light; NIR + PRC + RT: Prussian blue NPs-agarose hydrogel, NIR light and high-energy radiation (2 Gy). Adapted with permission from ref. 173. Copyright 2021, Elsevier B.V.





## 5. Conclusion and remarks for the future

In this review, the application of injectable hydrogels for mediating nanomaterials' cancer combinatorial-PTT was analyzed.

The use of injectable hydrogels for the local delivery of nanomaterials and/or other agents directly into the tumor ensured appropriate levels of these compounds at the target site while sparing other tissues from off-target toxicity. This is crucial to overcome the limitations associated with the systemic administration of anti-cancer therapies. These injectable hydrogels have been assembled using a myriad of natural (*e.g.*, chitosan, alginate, cellulose, HA) and synthetic (*e.g.*, Pluronic F127, PC10A, PEG) polymers. In this regard, the polymers' selection was revealed to be of utmost importance since it affected the properties of the attained injectable hydrogels and also directed the hydrogel's crosslinking mechanism (physical, chemical or hybrid). Just as important, injectable hydrogels were also designed to be responsive to different external and internal stimuli (*e.g.*, pH, enzymes, magnetic field, light), which assisted in the assembly/disassembly process, degradation, and release of the loaded nanomaterials/therapeutic agents, ultimately providing a path for a more controlled therapy.

The standalone use of injectable hydrogels incorporating nanomaterials aimed at cancer PTT has proved to be capable of good *in vivo* outcomes. In this regard, some hydrogel formulations were capable of inducing tumor eradication or regression after NIR laser irradiation. However, the vast majority of the analyzed injectable hydrogels containing nanomaterials intended for PTT only prompted a reduction of the tumor's growth (Table 1). Such outcome is likely multifactorial, highlighting the limitations of standalone PTT (*e.g.*, penetration limit of NIR light, heterogeneous heat transfer in the tumor mass).<sup>199,200</sup>

In order to improve the therapeutic outcome, injectable hydrogels containing photothermal nano-agents were combined with other modalities: PDT, chemotherapy, immunotherapy, radiotherapy. These combinatorial approaches aimed to overcome the limitations of PTT and of the other standalone therapies, leading to synergistic outcomes. Among the different combinatorial strategies analyzed (Table 2), injectable hydrogels containing nanomaterials for PTT combined with PDT and chemotherapy were by far the most explored. In fact, the application of injectable hydrogels for combinatorial-PTT led to an increase in the levels of tumor eradications and regressions. In these works, the respective standalone therapies mostly prompted a reduction in the tumor's growth, thus emphasizing the enhanced outcome that arises from the injectable hydrogel combinatorial-PTT.

The number of publications related to injectable hydrogels for cancer PTT and combinatorial-PTT has clearly been growing in the last 5 years. So far, several clinical trials using injectable hydrogels for cancer-related applications have been proposed/completed (*e.g.*, ClinicalTrials.gov Identifiers:

NCT03713021, NCT01538628, NCT03125226, NCT05224869). Furthermore, the use of hydrogels in numerous biomedical-related applications has increased, their market being estimated to generate revenues of 31.4 billion USD by 2027.<sup>201,202</sup>

Notwithstanding, in order to accelerate the translation of injectable hydrogels, it is crucial to address the issues related to their sterilization, scale-up and stability during storage. In this regard, the incorporation of anti-microbial agents into the hydrogels (*e.g.*, silver nanoparticles, chitosan) may reduce the risk of infection after their injection. Additionally, the use of non-toxic elements in the injectable hydrogels' assembly may accelerate the laborious and time-consuming purification steps. The fabrication of the injectable hydrogels' precursor solutions in state-of-the-art equipment may also ease the scale-up processes. In turn, strictly controlling the handling and storage conditions (*e.g.*, temperature, moisture, pH, exposure to radiation) of the injectable hydrogels and respective precursor solutions is fundamental to improving their stability during storage.

Moreover, the gelation time of some injectable hydrogels could be improved, since this parameter is crucial to efficiently confine the therapeutics in the tumor zone. In this context, the optimization of the polymer's features (*e.g.*, molecular weight, polydispersity, viscosity) and crosslinking strategies (*e.g.*, crosslinking degree, combination of physical and chemical crosslinking) may endow injectable hydrogels with an even faster gelling time that will prevent leakage of the therapeutics to undesired sites. Another challenge is related to the release kinetics of the loaded therapeutic agents from the injectable hydrogels. In this regard, the production of hierarchically organized injectable hydrogel systems with logical and scheduled release through layered degradation is an appealing strategy.

Finally, appropriate selection of the biological models/assays for screening the efficacy and safety of the injectable hydrogels for cancer combinatorial-PTT is also of critical importance. Besides the classical *in vitro* models, the adoption of advanced screening toolsets based on 3D cultures (*e.g.*, spheroids<sup>203</sup>) or organ-on-a-chip<sup>204</sup> could enable a better *in vitro* evaluation of the injectable hydrogels' performance. Such screening using these state-of-the-art models could contribute to the discovery of formulations with greater chances of performing *in vivo* as well as the ability to discard earlier those that will yield unsatisfactory results.

On the other hand, the long-term biodegradability of the injectable hydrogels for combinatorial-PTT is also a parameter that deserves further investigation and fine-tuning. Firstly, most studies dedicated to this matter only analyze the short-term biocompatibility in small animal models (*e.g.*, mice). In this regard, assessing the long-term biocompatibility of the injectable hydrogels is of utmost importance for their future clinical translation. Furthermore, it is also crucial to perform such analyses in both small- and large-scale animal models (*e.g.*, non-human primates). In turn, the biocompatibility of the injectable hydrogels may also be enhanced through the use of biodegradable materials in their formulation, such as natural polymers or synthetic polymers engineered with bio-



logically labile sub-units. On this subject, favoring the use of photothermal agents that are easily decomposed (*e.g.*, biodegradable nanoparticles loading NIR light-absorbing small molecules) or that are rapidly cleared through renal filtration (*i.e.*, nanostructures with a size below 5 nm) may also contribute to the translation of injectable hydrogels for combinatorial-PTT.

Overall, the continuous investigation of injectable hydrogels for nanomaterials-mediated combinatorial-PTT brings forward the possibility of attaining a multifunctional system for an improved and selective anti-cancer treatment.

## Author contributions

Rita Lima-Sousa: conceptualization, investigation, writing – original draft; Cátia G. Alves: writing – review & editing; Bruna L. Melo: writing – review & editing; Francisco J. P. Costa: writing – review & editing; Micaela Nave: writing – review & editing; André F. Moreira: writing – review & editing; António G. Mendonça: writing – review & editing, supervision; Ilídio J. Correia: project administration, funding acquisition, supervision, writing – review & editing; Duarte de Melo-Diogo: conceptualization, project administration, funding acquisition, supervision, writing – review & editing.

## Conflicts of interest

There are no conflicts to declare.

## Acknowledgements

This work was developed within the scope of the CICS-UBI projects UIDB/00709/2020 and UIDP/00709/2020, financed by National funds through the Portuguese Foundation for Science and Technology (FCT)/MCTES. The funding from POCI-01-0145-FEDER-031462, PTDC/BTA-BTA/0696/2020 and 2022.06320.PTDC is also acknowledged. Duarte de Melo-Diogo acknowledges FCT for the financial support given through a Junior Researcher contract (2021.00590.CEECIND). Rita Lima-Sousa, Cátia G. Alves and Bruna L. Melo acknowledge funding from individual Ph.D. fellowships from FCT (SFRH/BD/144922/2019, SFRH/BD/145386/2019 and 2021.06044.BD).

## References

- 1 H. Sung, J. Ferlay, R. L. Siegel, M. Laversanne, I. Soerjomataram, A. Jemal, *et al.*, Global Cancer Statistics 2020: GLOBOCAN Estimates of Incidence and Mortality Worldwide for 36 Cancers in 185 Countries, *CA-Cancer J. Clin.*, 2021, **71**(3), 209–249, DOI: [10.3322/caac.21660](https://doi.org/10.3322/caac.21660).
- 2 C. Mattiuzzi and G. Lippi, Current Cancer Epidemiology, *J. Epidemiol. Glob. Health*, 2019, **9**(4), 217–222, DOI: [10.2991/jegh.k.191008.001](https://doi.org/10.2991/jegh.k.191008.001).
- 3 V. Schirrmacher, From chemotherapy to biological therapy: A review of novel concepts to reduce the side effects of systemic cancer treatment (Review), *Int. J. Oncol.*, 2019, **54**(2), 407–419, DOI: [10.3892/ijo.2018.4661](https://doi.org/10.3892/ijo.2018.4661).
- 4 Z. Cheng, M. Li, R. Dey and Y. Chen, Nanomaterials for cancer therapy: current progress and perspectives, *J. Hematol. Oncol.*, 2021, **14**(1), 85, DOI: [10.1186/s13045-021-01096-0](https://doi.org/10.1186/s13045-021-01096-0).
- 5 E. B. Yahya and A. M. Alqadhi, Recent trends in cancer therapy: A review on the current state of gene delivery, *Life Sci.*, 2021, **269**, 119087, DOI: [10.1016/j.lfs.2021.119087](https://doi.org/10.1016/j.lfs.2021.119087).
- 6 G. Cirillo, U. G. Spizzirri, M. Curcio, F. P. Nicoletta and F. Iemma, Injectable Hydrogels for Cancer Therapy over the Last Decade, *Pharmaceutics*, 2019, **11**(9), 486, DOI: [10.3390/pharmaceutics11090486](https://doi.org/10.3390/pharmaceutics11090486).
- 7 H. Zhang and J. Chen, Current status and future directions of cancer immunotherapy, *J. Cancer*, 2018, **9**(10), 1773–1781, DOI: [10.7150/jca.24577](https://doi.org/10.7150/jca.24577).
- 8 D. de Melo-Diogo, C. Pais-Silva, D. R. Dias, A. F. Moreira and I. J. Correia, Strategies to Improve Cancer Photothermal Therapy Mediated by Nanomaterials, *Adv. Healthcare Mater.*, 2017, **6**(10), 1700073, DOI: [10.1002/adhm.201700073](https://doi.org/10.1002/adhm.201700073).
- 9 N. Fernandes, C. F. Rodrigues, A. F. Moreira and I. J. Correia, Overview of the application of inorganic nanomaterials in cancer photothermal therapy, *Biomater. Sci.*, 2020, **8**(11), 2990–3020, DOI: [10.1039/d0bm00222d](https://doi.org/10.1039/d0bm00222d).
- 10 D. de Melo-Diogo, R. Lima-Sousa, C. G. Alves and I. J. Correia, Graphene family nanomaterials for application in cancer combination photothermal therapy, *Biomater. Sci.*, 2019, **7**(9), 3534–3551, DOI: [10.1039/c9bm00577c](https://doi.org/10.1039/c9bm00577c).
- 11 J. Chen, C. Ning, Z. Zhou, P. Yu, Y. Zhu, G. Tan, *et al.*, Nanomaterials as photothermal therapeutic agents, *Prog. Mater. Sci.*, 2019, **99**, 1–26, DOI: [10.1016/j.pmatsci.2018.07.005](https://doi.org/10.1016/j.pmatsci.2018.07.005).
- 12 A. V. P. Kumar, S. K. Dubey, S. Tiwari, A. Puri, S. Hejmady, B. Gorain, *et al.*, Recent advances in nanoparticles mediated photothermal therapy induced tumor regression, *Int. J. Pharm.*, 2021, **606**, 120848, DOI: [10.1016/j.ijpharm.2021.120848](https://doi.org/10.1016/j.ijpharm.2021.120848).
- 13 H. S. Han and K. Y. Choi, Advances in Nanomaterial-Mediated Photothermal Cancer Therapies: Toward Clinical Applications, *Biomedicines*, 2021, **9**(3), 305, DOI: [10.3390/biomedicines9030305](https://doi.org/10.3390/biomedicines9030305).
- 14 L. Zhao, Y. Liu, R. Xing and X. Yan, Supramolecular Photothermal Effects: A Promising Mechanism for Efficient Thermal Conversion, *Angew. Chem., Int. Ed.*, 2020, **59**(10), 3793–3801, DOI: [10.1002/anie.201909825](https://doi.org/10.1002/anie.201909825).
- 15 L. Zhao, X. Zhang, X. Wang, X. Guan, W. Zhang and J. Ma, Recent advances in selective photothermal therapy of tumor, *J. Nanobiotechnol.*, 2021, **19**(1), 335, DOI: [10.1186/s12951-021-01080-3](https://doi.org/10.1186/s12951-021-01080-3).
- 16 A. Granja, R. Lima-Sousa, C. G. Alves, D. de Melo-Diogo, C. Nunes, C. T. Sousa, *et al.*, Multifunctional targeted



- solid lipid nanoparticles for combined photothermal therapy and chemotherapy of breast cancer, *Biomater. Adv.*, 2023, **151**, 213443, DOI: [10.1016/j.bioadv.2023.213443](https://doi.org/10.1016/j.bioadv.2023.213443).
- 17 C. Song, F. Li, X. Guo, W. Chen, C. Dong, J. Zhang, *et al.*, Gold nanostars for cancer cell-targeted SERS-imaging and NIR light-triggered plasmonic photothermal therapy (PPTT) in the first and second biological windows, *J. Mater. Chem. B*, 2019, **7**(12), 2001–2008, DOI: [10.1039/c9tb00061e](https://doi.org/10.1039/c9tb00061e).
  - 18 B. Zhang, H. Wang, S. Shen, X. She, W. Shi, J. Chen, *et al.*, Fibrin-targeting peptide CREKA-conjugated multi-walled carbon nanotubes for self-amplified photothermal therapy of tumor, *Biomaterials*, 2016, **79**, 46–55, DOI: [10.1016/j.biomaterials.2015.11.061](https://doi.org/10.1016/j.biomaterials.2015.11.061).
  - 19 M. M. Leitão, C. G. Alves, D. de Melo-Diogo, R. Lima-Sousa, A. F. Moreira and I. J. Correia, Sulfobetaine methacrylate-functionalized graphene oxide-IR780 nanohybrids aimed at improving breast cancer phototherapy, *RSC Adv.*, 2020, **10**(63), 38621–38630, DOI: [10.1039/d0ra07508f](https://doi.org/10.1039/d0ra07508f).
  - 20 R. Lima-Sousa, C. G. Alves, B. L. Melo, A. F. Moreira, A. G. Mendonça, I. J. Correia, *et al.*, Poly(2-ethyl-2-oxazoline) functionalized reduced graphene oxide: Optimization of the reduction process using dopamine and application in cancer photothermal therapy, *Mater. Sci. Eng., C*, 2021, **130**, 112468, DOI: [10.1016/j.msec.2021.112468](https://doi.org/10.1016/j.msec.2021.112468).
  - 21 X. Zhang, J. Wu, G. R. Williams, S. Niu, Q. Qian and L. M. Zhu, Functionalized MoS<sub>2</sub>-nanosheets for targeted drug delivery and chemo-photothermal therapy, *Colloids Surf., B*, 2019, **173**, 101–108, DOI: [10.1016/j.colsurfb.2018.09.048](https://doi.org/10.1016/j.colsurfb.2018.09.048).
  - 22 J. T. Wang, W. Zhang, W. B. Wang, Y. J. Wu, L. Zhou and F. Cao, One-pot bottom-up fabrication of biocompatible PEGylated WS<sub>2</sub> nanoparticles for CT-guided photothermal therapy of tumors in vivo, *Biochem. Biophys. Res. Commun.*, 2019, **511**(3), 587–591, DOI: [10.1016/j.bbrc.2019.01.009](https://doi.org/10.1016/j.bbrc.2019.01.009).
  - 23 S. Li, W. Zhang, R. Xing, C. Yuan, H. Xue and X. Yan, Supramolecular Nanofibrils Formed by Coassembly of Clinically Approved Drugs for Tumor Photothermal Immunotherapy, *Adv. Mater.*, 2021, **33**(21), e2100595, DOI: [10.1002/adma.202100595](https://doi.org/10.1002/adma.202100595).
  - 24 C. G. Alves, D. de Melo-Diogo, R. Lima-Sousa and I. J. Correia, IR780 loaded sulfobetaine methacrylate-functionalized albumin nanoparticles aimed for enhanced breast cancer phototherapy, *Int. J. Pharm.*, 2020, **582**, 119346, DOI: [10.1016/j.ijpharm.2020.119346](https://doi.org/10.1016/j.ijpharm.2020.119346).
  - 25 Y. Liang, W. Guo, C. Li, G. Shen, H. Tan, P. Sun, *et al.*, Tumor-Targeted Polydopamine-Based Nanoparticles for Multimodal Mapping Following Photothermal Therapy of Metastatic Lymph Nodes, *Int. J. Nanomed.*, 2022, **17**, 4659–4675, DOI: [10.2147/ijn.s367975](https://doi.org/10.2147/ijn.s367975).
  - 26 R. Chang, Q. Zou, L. Zhao, Y. Liu, R. Xing and X. Yan, Amino-Acid-Encoded Supramolecular Photothermal Nanomedicine for Enhanced Cancer Therapy, *Adv. Mater.*, 2022, **34**(16), e2200139, DOI: [10.1002/adma.202200139](https://doi.org/10.1002/adma.202200139).
  - 27 C. G. Alves, R. Lima-Sousa, B. L. Melo, P. Ferreira, A. F. Moreira, I. J. Correia, *et al.*, Poly(2-ethyl-2-oxazoline)-IR780 conjugate nanoparticles for breast cancer phototherapy, *Nanomedicine*, 2022, **17**(27), 2057–2072, DOI: [10.2217/nmm-2022-0218](https://doi.org/10.2217/nmm-2022-0218).
  - 28 Y. Shi, R. van der Meel, X. Chen and T. Lammers, The EPR effect and beyond: Strategies to improve tumor targeting and cancer nanomedicine treatment efficacy, *Theranostics*, 2020, **10**(17), 7921–7924, DOI: [10.7150/thno.49577](https://doi.org/10.7150/thno.49577).
  - 29 V. Sheth, L. Wang, R. Bhattacharya, P. Mukherjee and S. Wilhelm, Strategies for Delivering Nanoparticles across Tumor Blood Vessels, *Adv. Funct. Mater.*, 2021, **31**(8), 2007363, DOI: [10.1002/adfm.202007363](https://doi.org/10.1002/adfm.202007363).
  - 30 S. Wilhelm, A. J. Tavares, Q. Dai, S. Ohta, J. Audet, H. F. Dvorak, *et al.*, Analysis of nanoparticle delivery to tumours, *Nat. Rev. Mater.*, 2016, **1**(5), 16014, DOI: [10.1038/natrevmats.2016.14](https://doi.org/10.1038/natrevmats.2016.14).
  - 31 D. Sun, S. Zhou and W. Gao, What Went Wrong with Anticancer Nanomedicine Design and How to Make It Right, *ACS Nano*, 2020, **14**(10), 12281–12290, DOI: [10.1021/acsnano.9b09713](https://doi.org/10.1021/acsnano.9b09713).
  - 32 F. Danhier, To exploit the tumor microenvironment: Since the EPR effect fails in the clinic, what is the future of nanomedicine?, *J. Controlled Release*, 2016, **244**(Pt A), 108–121, DOI: [10.1016/j.jconrel.2016.11.015](https://doi.org/10.1016/j.jconrel.2016.11.015).
  - 33 A. F. Moreira, C. F. Rodrigues, T. A. Jacinto, S. P. Miguel, E. C. Costa and I. J. Correia, Microneedle-based delivery devices for cancer therapy: A review, *Pharmacol. Res.*, 2019, **148**, 104438, DOI: [10.1016/j.phrs.2019.104438](https://doi.org/10.1016/j.phrs.2019.104438).
  - 34 D. Y. Fan, Y. Tian and Z. J. Liu, Injectable Hydrogels for Localized Cancer Therapy, *Front. Chem.*, 2019, **7**, 675, DOI: [10.3389/fchem.2019.00675](https://doi.org/10.3389/fchem.2019.00675).
  - 35 Z. Huang, Z. Tian, M. Zhu, C. Wu and Y. Zhu, Recent Advances in Biomaterial Scaffolds for Integrative Tumor Therapy and Bone Regeneration, *Adv. Ther.*, 2021, **4**(3), 2000212, DOI: [10.1002/adtp.202000212](https://doi.org/10.1002/adtp.202000212).
  - 36 C. Y. X. Chua, J. Ho, S. Demaria, M. Ferrari and A. Grattoni, Emerging Technologies for Local Cancer Treatment, *Adv. Ther.*, 2020, **3**(9), 2000027, DOI: [10.1002/adtp.202000027](https://doi.org/10.1002/adtp.202000027).
  - 37 M. Mohammadi, M. Karimi, B. Malaekheh-Nikouei, M. Torkashvand and M. Alibolandi, Hybrid in situ-forming injectable hydrogels for local cancer therapy, *Int. J. Pharm.*, 2022, **616**, 121534, DOI: [10.1016/j.ijpharm.2022.121534](https://doi.org/10.1016/j.ijpharm.2022.121534).
  - 38 W. Park, H. Shin, B. Choi, W.-K. Rhim, K. Na and D. Keun Han, Advanced hybrid nanomaterials for biomedical applications, *Prog. Mater. Sci.*, 2020, **114**, 100686, DOI: [10.1016/j.pmatsci.2020.100686](https://doi.org/10.1016/j.pmatsci.2020.100686).
  - 39 G. R. Shin, H. E. Kim, J. H. Kim, S. Choi and M. S. Kim, Advances in Injectable In Situ-Forming Hydrogels for Intratumoral Treatment, *Pharmaceutics*, 2021, **13**(11), 1953, DOI: [10.3390/pharmaceutics13111953](https://doi.org/10.3390/pharmaceutics13111953).
  - 40 V. K. A. Devi, R. Shyam, A. Palaniappan, A. K. Jaiswal, T. H. Oh and A. J. Nathanael, Self-Healing Hydrogels:



- Preparation, Mechanism and Advancement in Biomedical Applications, *Polymers*, 2021, **13**(21), 3782, DOI: [10.3390/polym13213782](https://doi.org/10.3390/polym13213782).
- 41 S. Lin, Y. Cao, J. Chen, Z. Tian and Y. Zhu, Recent advances in microneedles for tumor therapy and diagnosis, *Appl. Mater. Today*, 2021, **23**, 101036, DOI: [10.1016/j.apmt.2021.101036](https://doi.org/10.1016/j.apmt.2021.101036).
- 42 K.-Y. Qian, Y. Song, X. Yan, L. Dong, J. Xue, Y. Xu, *et al.*, Injectable ferrimagnetic silk fibroin hydrogel for magnetic hyperthermia ablation of deep tumor, *Biomaterials*, 2020, **259**, 120299, DOI: [10.1016/j.biomaterials.2020.120299](https://doi.org/10.1016/j.biomaterials.2020.120299).
- 43 R. Xing, Y. Liu, Q. Zou and X. Yan, Self-assembled injectable biomolecular hydrogels towards phototherapy, *Nanoscale*, 2019, **11**(46), 22182–22195, DOI: [10.1039/C9NR06266A](https://doi.org/10.1039/C9NR06266A).
- 44 R. Lima-Sousa, D. de Melo-Diogo, C. G. Alves, C. S. D. Cabral, S. P. Miguel, A. G. Mendonça, *et al.*, Injectable in situ forming thermo-responsive graphene based hydrogels for cancer chemo-photothermal therapy and NIR light-enhanced antibacterial applications, *Mater. Sci. Eng., C*, 2020, **117**, 111294, DOI: [10.1016/j.msec.2020.111294](https://doi.org/10.1016/j.msec.2020.111294).
- 45 P. Huang, H. Song, Y. Zhang, J. Liu, J. Zhang, W. Wang, *et al.*, Bridging the Gap between Macroscale Drug Delivery Systems and Nanomedicines: A Nanoparticle-Assembled Thermosensitive Hydrogel for Peritumoral Chemotherapy, *ACS Appl. Mater. Interfaces*, 2016, **8**(43), 29323–29333, DOI: [10.1021/acsami.6b10416](https://doi.org/10.1021/acsami.6b10416).
- 46 W. Wang, L. Deng, S. Xu, X. Zhao, N. Lv, G. Zhang, *et al.*, A reconstituted “two into one” thermosensitive hydrogel system assembled by drug-loaded amphiphilic copolymer nanoparticles for the local delivery of paclitaxel, *J. Mater. Chem. B*, 2013, **1**(4), 552–563, DOI: [10.1039/c2tb00068g](https://doi.org/10.1039/c2tb00068g).
- 47 A. Gaowa, T. Horibe, M. Kohno, K. Sato, H. Harada, M. Hiraoka, *et al.*, Combination of hybrid peptide with biodegradable gelatin hydrogel for controlled release and enhancement of anti-tumor activity in vivo, *J. Controlled Release*, 2014, **176**, 1–7, DOI: [10.1016/j.jconrel.2013.12.021](https://doi.org/10.1016/j.jconrel.2013.12.021).
- 48 J. H. Lee, Injectable hydrogels delivering therapeutic agents for disease treatment and tissue engineering, *Biomater. Res.*, 2018, **22**, 27, DOI: [10.1186/s40824-018-0138-6](https://doi.org/10.1186/s40824-018-0138-6).
- 49 X. Fang, C. Wang, S. Zhou, P. Cui, H. Hu, X. Ni, *et al.*, Hydrogels for Antitumor and Antibacterial Therapy, *Gels*, 2022, **8**(5), 315, DOI: [10.3390/gels8050315](https://doi.org/10.3390/gels8050315).
- 50 J. M. Alonso, J. Andrade Del Olmo, R. Perez Gonzalez and V. Saez-Martinez, Injectable Hydrogels: From Laboratory to Industrialization, *Polymers*, 2021, **13**(4), 650, DOI: [10.3390/polym13040650](https://doi.org/10.3390/polym13040650).
- 51 I. J. Sabino, R. Lima-Sousa, C. G. Alves, B. L. Melo, A. F. Moreira, I. J. Correia, *et al.*, Injectable in situ forming hydrogels incorporating dual-nanoparticles for chemo-photothermal therapy of breast cancer cells, *Int. J. Pharm.*, 2021, **600**, 120510, DOI: [10.1016/j.ijpharm.2021.120510](https://doi.org/10.1016/j.ijpharm.2021.120510).
- 52 E. Jalalvandi and A. Shavandi, Shear thinning/self-healing hydrogel based on natural polymers with secondary photocrosslinking for biomedical applications, *J. Mech. Behav. Biomed. Mater.*, 2019, **90**, 191–201, DOI: [10.1016/j.jmbbm.2018.10.009](https://doi.org/10.1016/j.jmbbm.2018.10.009).
- 53 F. Rizzo and N. S. Kehr, Recent Advances in Injectable Hydrogels for Controlled and Local Drug Delivery, *Adv. Healthcare Mater.*, 2021, **10**(1), e2001341, DOI: [10.1002/adhm.202001341](https://doi.org/10.1002/adhm.202001341).
- 54 S. Uman, A. Dhand and J. A. Burdick, Recent advances in shear-thinning and self-healing hydrogels for biomedical applications, *J. Appl. Polym. Sci.*, 2020, **137**(25), 48668, DOI: [10.1002/app.48668](https://doi.org/10.1002/app.48668).
- 55 Y. Tu, N. Chen, C. Li, H. Liu, R. Zhu, S. Chen, *et al.*, Advances in injectable self-healing biomedical hydrogels, *Acta Biomater.*, 2019, **90**, 1–20, DOI: [10.1016/j.actbio.2019.03.057](https://doi.org/10.1016/j.actbio.2019.03.057).
- 56 S. Yu, C. He and X. Chen, Injectable Hydrogels as Unique Platforms for Local Chemotherapeutics-Based Combination Antitumor Therapy, *Macromol. Biosci.*, 2018, **18**(12), e1800240, DOI: [10.1002/mabi.201800240](https://doi.org/10.1002/mabi.201800240).
- 57 T. Hozumi, T. Kageyama, S. Ohta, J. Fukuda and T. Ito, Injectable Hydrogel with Slow Degradability Composed of Gelatin and Hyaluronic Acid Cross-Linked by Schiff's Base Formation, *Biomacromolecules*, 2018, **19**(2), 288–297, DOI: [10.1021/acs.biomac.7b01133](https://doi.org/10.1021/acs.biomac.7b01133).
- 58 Z. M. Khan, E. Wilts, E. Vlaisavljevich, T. E. Long and S. S. Verbridge, Characterization and structure-property relationships of an injectable thiol-Michael addition hydrogel toward compatibility with glioblastoma therapy, *Acta Biomater.*, 2022, **144**, 266–278, DOI: [10.1016/j.actbio.2022.03.016](https://doi.org/10.1016/j.actbio.2022.03.016).
- 59 K. Xu, H. Yao, D. Fan, L. Zhou and S. Wei, Hyaluronic acid thiol modified injectable hydrogel: Synthesis, characterization, drug release, cellular drug uptake and anticancer activity, *Carbohydr. Polym.*, 2021, **254**, 117286, DOI: [10.1016/j.carbpol.2020.117286](https://doi.org/10.1016/j.carbpol.2020.117286).
- 60 Y.-J. Jo, M. Gulfam, S.-H. Jo, Y.-S. Gal, C.-W. Oh, S.-H. Park, *et al.*, Multi-stimuli responsive hydrogels derived from hyaluronic acid for cancer therapy application, *Carbohydr. Polym.*, 2022, **286**, 119303, DOI: [10.1016/j.carbpol.2022.119303](https://doi.org/10.1016/j.carbpol.2022.119303).
- 61 Y. Wang, S. Wang, W. Hu, F. Su, F. Liu and S. Li, In situ photo-crosslinked hydrogels prepared from acrylated 4-arm-poly(ethylene glycol)-poly( $\epsilon$ -caprolactone) block copolymers for local cancer therapy, *Polym. Adv. Technol.*, 2022, **33**(8), 2620–2631, DOI: [10.1002/pat.5718](https://doi.org/10.1002/pat.5718).
- 62 V. Crescenzi, L. Cornelio, C. Di Meo, S. Nardecchia and R. Lamanna, Novel Hydrogels via Click Chemistry: Synthesis and Potential Biomedical Applications, *Biomacromolecules*, 2007, **8**(6), 1844–1850, DOI: [10.1021/bm0700800](https://doi.org/10.1021/bm0700800).
- 63 F. J. P. Costa, M. Nave, R. Lima-Sousa, C. G. Alves, B. L. Melo, I. J. Correia, *et al.*, Development of Thiol-Maleimide hydrogels incorporating graphene-based nanomaterials for cancer chemo-photothermal therapy,





- Int. J. Pharm.*, 2023, **635**, 122713, DOI: [10.1016/j.ijpharm.2023.122713](https://doi.org/10.1016/j.ijpharm.2023.122713).
- 64 D. C. Tuncaboylu, A. Argun, M. Sahin, M. Sari and O. Okay, Structure optimization of self-healing hydrogels formed via hydrophobic interactions, *Polymer*, 2012, **53**(24), 5513–5522, DOI: [10.1016/j.polymer.2012.10.015](https://doi.org/10.1016/j.polymer.2012.10.015).
- 65 C. Wu, J. Zhao, F. Hu, Y. Zheng, H. Yang, S. Pan, *et al.*, Design of injectable agar-based composite hydrogel for multi-mode tumor therapy, *Carbohydr. Polym.*, 2018, **180**, 112–121, DOI: [10.1016/j.carbpol.2017.10.024](https://doi.org/10.1016/j.carbpol.2017.10.024).
- 66 M. Fathi, M. Alami-Milani, M. H. Geranmayeh, J. Barar, H. Erfan-Niya and Y. Omid, Dual thermo- and pH-sensitive injectable hydrogels of chitosan/(poly(N-isopropylacrylamide-co-itaconic acid)) for doxorubicin delivery in breast cancer, *Int. J. Biol. Macromol.*, 2019, **128**, 957–964, DOI: [10.1016/j.ijbiomac.2019.01.122](https://doi.org/10.1016/j.ijbiomac.2019.01.122).
- 67 X. Jiang, F. Zeng, X. Yang, C. Jian, L. Zhang, A. Yu, *et al.*, Injectable self-healing cellulose hydrogel based on host-guest interactions and acylhydrazone bonds for sustained cancer therapy, *Acta Biomater.*, 2022, **141**, 102–113, DOI: [10.1016/j.actbio.2021.12.036](https://doi.org/10.1016/j.actbio.2021.12.036).
- 68 A. Baral, S. Roy, A. Dehsorkhi, I. W. Hamley, S. Mohapatra, S. Ghosh, *et al.*, Assembly of an injectable noncytotoxic peptide-based hydrogelator for sustained release of drugs, *Langmuir*, 2014, **30**(3), 929–936, DOI: [10.1021/la4043638](https://doi.org/10.1021/la4043638).
- 69 B. L. Melo, R. Lima-Sousa, C. G. Alves, A. F. Moreira, I. J. Correia and D. de Melo-Diogo, Chitosan-based injectable in situ forming hydrogels containing dopamine-reduced graphene oxide and resveratrol for breast cancer chemo-photothermal therapy, *Biochem. Eng. J.*, 2022, **185**, 108529, DOI: [10.1016/j.bej.2022.108529](https://doi.org/10.1016/j.bej.2022.108529).
- 70 F. Andrade, M. M. Roca-Melendres, E. F. Durán-Lara, D. Rafael and S. Schwartz Jr., Stimuli-Responsive Hydrogels for Cancer Treatment: The Role of pH, Light, Ionic Strength and Magnetic Field, *Cancers*, 2021, **13**(5), 1164, DOI: [10.3390/cancers13051164](https://doi.org/10.3390/cancers13051164).
- 71 N. N. Ferreira, L. M. B. Ferreira, V. M. O. Cardoso, F. I. Boni, A. L. R. Souza and M. P. D. Gremião, Recent advances in smart hydrogels for biomedical applications: From self-assembly to functional approaches, *Eur. Polym. J.*, 2018, **99**, 117–133, DOI: [10.1016/j.eurpolymj.2017.12.004](https://doi.org/10.1016/j.eurpolymj.2017.12.004).
- 72 H. Xin and S. Naficy, Drug Delivery Based on Stimuli-Responsive Injectable Hydrogels for Breast Cancer Therapy: A Review, *Gels*, 2022, **8**(1), 45, DOI: [10.3390/gels8010045](https://doi.org/10.3390/gels8010045).
- 73 A. C. Marques, P. J. Costa, S. Velho and M. H. Amaral, Stimuli-responsive hydrogels for intratumoral drug delivery, *Drug Discovery Today*, 2021, **26**(10), 2397–2405, DOI: [10.1016/j.drudis.2021.04.012](https://doi.org/10.1016/j.drudis.2021.04.012).
- 74 Y. Chen, Y. Hao, Y. Huang, W. Wu, X. Liu, Y. Li, *et al.*, An Injectable, Near-Infrared Light-Responsive Click Cross-Linked Azobenzene Hydrogel for Breast Cancer Chemotherapy, *J. Biomed. Nanotechnol.*, 2019, **15**(9), 1923–1936, DOI: [10.1166/jbn.2019.2821](https://doi.org/10.1166/jbn.2019.2821).
- 75 S. Wang, H. Zheng, L. Zhou, F. Cheng, Z. Liu, H. Zhang, *et al.*, Injectable redox and light responsive MnO<sub>2</sub> hybrid hydrogel for simultaneous melanoma therapy and multi-drug-resistant bacteria-infected wound healing, *Biomaterials*, 2020, **260**, 120314, DOI: [10.1016/j.biomaterials.2020.120314](https://doi.org/10.1016/j.biomaterials.2020.120314).
- 76 M. Zhao, E. Bozzato, N. Joudiou, S. Ghiassinejad, F. Danhier, B. Gallez, *et al.*, Codelivery of paclitaxel and temozolomide through a photopolymerizable hydrogel prevents glioblastoma recurrence after surgical resection, *J. Controlled Release*, 2019, **309**, 72–81, DOI: [10.1016/j.jconrel.2019.07.015](https://doi.org/10.1016/j.jconrel.2019.07.015).
- 77 Q. Chen, X. Li, Y. Xie, W. Hu, Z. Cheng, H. Zhong, *et al.*, Alginate-azo/chitosan nanocapsules in vitro drug delivery for hepatic carcinoma cells: UV-stimulated decomposition and drug release based on trans-to-cis isomerization, *Int. J. Biol. Macromol.*, 2021, **187**, 214–222, DOI: [10.1016/j.ijbiomac.2021.07.119](https://doi.org/10.1016/j.ijbiomac.2021.07.119).
- 78 A. Kasiński, M. Zielińska-Pisklak, E. Oledzka and M. Sobczak, Smart Hydrogels - Synthetic Stimuli-Responsive Antitumor Drug Release Systems, *Int. J. Nanomed.*, 2020, **15**, 4541–4572, DOI: [10.2147/ijn.s248987](https://doi.org/10.2147/ijn.s248987).
- 79 L. Wang, B. Li, F. Xu, Z. Xu, D. Wei, Y. Feng, *et al.*, UV-crosslinkable and thermo-responsive chitosan hybrid hydrogel for NIR-triggered localized on-demand drug delivery, *Carbohydr. Polym.*, 2017, **174**, 904–914, DOI: [10.1016/j.carbpol.2017.07.013](https://doi.org/10.1016/j.carbpol.2017.07.013).
- 80 W. Xie, Q. Gao, Z. Guo, D. Wang, F. Gao, X. Wang, *et al.*, Injectable and Self-Healing Thermosensitive Magnetic Hydrogel for Asynchronous Control Release of Doxorubicin and Docetaxel to Treat Triple-Negative Breast Cancer, *ACS Appl. Mater. Interfaces*, 2017, **9**(39), 33660–33673, DOI: [10.1021/acsami.7b10699](https://doi.org/10.1021/acsami.7b10699).
- 81 B. Pourbadie, S. Y. Adlsadabad, N. Rahbariasr and A. Pourjavadi, Synthesis and characterization of dual light/temperature-responsive supramolecular injectable hydrogel based on host-guest interaction between azobenzene and starch-grafted  $\beta$ -cyclodextrin: Melanoma therapy with paclitaxel, *Carbohydr. Polym.*, 2023, **313**, 120667, DOI: [10.1016/j.carbpol.2023.120667](https://doi.org/10.1016/j.carbpol.2023.120667).
- 82 M. S. Gil, T. Thambi, V. H. G. Phan, S. H. Kim and D. S. Lee, Injectable hydrogel-incorporated cancer cell-specific cisplatin releasing nanogels for targeted drug delivery, *J. Mater. Chem. B*, 2017, **5**(34), 7140–7152, DOI: [10.1039/c7tb00873b](https://doi.org/10.1039/c7tb00873b).
- 83 Y. Luo, J. Li, Y. Hu, F. Gao, G. Pak-Heng Leung, F. Geng, *et al.*, Injectable thermo-responsive nano-hydrogel loading triptolide for the anti-breast cancer enhancement via localized treatment based on “two strikes” effects, *Acta Pharm. Sin. B*, 2020, **10**(11), 2227–2245, DOI: [10.1016/j.apsb.2020.05.011](https://doi.org/10.1016/j.apsb.2020.05.011).
- 84 L. Klouda and A. G. Mikos, Thermoresponsive hydrogels in biomedical applications, *Eur. J. Pharm. Biopharm.*, 2008, **68**(1), 34–45, DOI: [10.1016/j.ejpb.2007.02.025](https://doi.org/10.1016/j.ejpb.2007.02.025).
- 85 Y. Zheng, W. Wang, J. Zhao, C. Wu, C. Ye, M. Huang, *et al.*, Preparation of injectable temperature-sensitive chit-



- osan-based hydrogel for combined hyperthermia and chemotherapy of colon cancer, *Carbohydr. Polym.*, 2019, **222**, 115039, DOI: [10.1016/j.carbpol.2019.115039](https://doi.org/10.1016/j.carbpol.2019.115039).
- 86 J. Zhan, Y. Wu, H. Wang, J. Liu, Q. Ma, K. Xiao, *et al.*, An injectable hydrogel with pH-sensitive and self-healing properties based on 4armPEGDA and N-carboxyethyl chitosan for local treatment of hepatocellular carcinoma, *Int. J. Biol. Macromol.*, 2020, **163**, 1208–1222, DOI: [10.1016/j.ijbiomac.2020.07.008](https://doi.org/10.1016/j.ijbiomac.2020.07.008).
- 87 J. Qu, X. Zhao, P. X. Ma and B. Guo, pH-responsive self-healing injectable hydrogel based on N-carboxyethyl chitosan for hepatocellular carcinoma therapy, *Acta Biomater.*, 2017, **58**, 168–180, DOI: [10.1016/j.actbio.2017.06.001](https://doi.org/10.1016/j.actbio.2017.06.001).
- 88 Q. Yao, L. Kou, Y. Tu and L. Zhu, MMP-Responsive ‘Smart’ Drug Delivery and Tumor Targeting, *Trends Pharmacol. Sci.*, 2018, **39**(8), 766–781, DOI: [10.1016/j.tips.2018.06.003](https://doi.org/10.1016/j.tips.2018.06.003).
- 89 N. Yadav, M. K. Chauhan and V. S. Chauhan, Short to ultrashort peptide-based hydrogels as a platform for biomedical applications, *Biomater. Sci.*, 2020, **8**(1), 84–100, DOI: [10.1039/c9bm01304k](https://doi.org/10.1039/c9bm01304k).
- 90 H. Tan, H. Li, J. P. Rubin and K. G. Marra, Controlled gelation and degradation rates of injectable hyaluronic acid-based hydrogels through a double crosslinking strategy, *J. Tissue Eng. Regener. Med.*, 2011, **5**(10), 790–797, DOI: [10.1002/term.378](https://doi.org/10.1002/term.378).
- 91 W. Li, C. Tao, J. Wang, Y. Le and J. Zhang, MMP-responsive in situ forming hydrogel loaded with doxorubicin-encapsulated biodegradable micelles for local chemotherapy of oral squamous cell carcinoma, *RSC Adv.*, 2019, **9**(54), 31264–31273, DOI: [10.1039/c9ra04343h](https://doi.org/10.1039/c9ra04343h).
- 92 D. Jaque, L. Martínez Maestro, B. del Rosal, P. Haro-Gonzalez, A. Benayas, J. L. Plaza, *et al.*, Nanoparticles for photothermal therapies, *Nanoscale*, 2014, **6**(16), 9494–9530, DOI: [10.1039/C4NR00708E](https://doi.org/10.1039/C4NR00708E).
- 93 X. Zhang, L.-Y. Xia, X. Chen, Z. Chen and F.-G. Wu, Hydrogel-based phototherapy for fighting cancer and bacterial infection, *Sci. China Mater.*, 2017, **60**(6), 487–503, DOI: [10.1007/s40843-017-9025-3](https://doi.org/10.1007/s40843-017-9025-3).
- 94 K. F. Chu and D. E. Dupuy, Thermal ablation of tumours: biological mechanisms and advances in therapy, *Nat. Rev. Cancer*, 2014, **14**(3), 199–208, DOI: [10.1038/nrc3672](https://doi.org/10.1038/nrc3672).
- 95 Y. J. Hou, X. X. Yang, R. Q. Liu, D. Zhao, C. X. Guo, A. C. Zhu, *et al.*, Pathological Mechanism of Photodynamic Therapy and Photothermal Therapy Based on Nanoparticles, *Int. J. Nanomed.*, 2020, **15**, 6827–6838, DOI: [10.2147/ij.n.s269321](https://doi.org/10.2147/ij.n.s269321).
- 96 Q. Hu, Z. Huang, Y. Duan, Z. Fu and L. Bin, Reprogramming Tumor Microenvironment with Photothermal Therapy, *Bioconjugate Chem.*, 2020, **31**(5), 1268–1278, DOI: [10.1021/acs.bioconjchem.0c00135](https://doi.org/10.1021/acs.bioconjchem.0c00135).
- 97 M. Nikfarjam, C. Malcontenti-Wilson and C. Christophi, Focal hyperthermia produces progressive tumor necrosis independent of the initial thermal effects, *J. Gastrointest. Surg.*, 2005, **9**(3), 410–417, DOI: [10.1016/j.gassur.2004.07.008](https://doi.org/10.1016/j.gassur.2004.07.008).
- 98 G. Y. Yi, M. J. Kim, H. I. Kim, J. Park and S. H. Baek, Hyperthermia Treatment as a Promising Anti-Cancer Strategy: Therapeutic Targets, Perspective Mechanisms and Synergistic Combinations in Experimental Approaches, *Antioxidants*, 2022, **11**(4), 625, DOI: [10.3390/antiox11040625](https://doi.org/10.3390/antiox11040625).
- 99 B. Hildebrandt, P. Wust, O. Ahlers, A. Dieing, G. Sreenivasa, T. Kerner, *et al.*, The cellular and molecular basis of hyperthermia, *Crit. Rev. Oncol. Hematol.*, 2002, **43**(1), 33–56, DOI: [10.1016/s1040-8428\(01\)00179-2](https://doi.org/10.1016/s1040-8428(01)00179-2).
- 100 A. L. Oei, L. E. M. Vriend, J. Crezee, N. A. P. Franken and P. M. Krawczyk, Effects of hyperthermia on DNA repair pathways: one treatment to inhibit them all, *Radiat. Oncol.*, 2015, **10**(1), 165, DOI: [10.1186/s13014-015-0462-0](https://doi.org/10.1186/s13014-015-0462-0).
- 101 N. van den Tempel, M. R. Horsman and R. Kanaar, Improving efficacy of hyperthermia in oncology by exploiting biological mechanisms, *Int. J. Hyperthermia*, 2016, **32**(4), 446–454, DOI: [10.3109/02656736.2016.1157216](https://doi.org/10.3109/02656736.2016.1157216).
- 102 M. Dunne, M. Regenold and C. Allen, Hyperthermia can alter tumor physiology and improve chemo- and radiotherapy efficacy, *Adv. Drug Delivery Rev.*, 2020, **163–164**, 98–124, DOI: [10.1016/j.addr.2020.07.007](https://doi.org/10.1016/j.addr.2020.07.007).
- 103 I. B. Slimen, T. Najjar, A. Ghram, H. Dabbebi, M. Ben Mrad and M. Abdrabbah, Reactive oxygen species, heat stress and oxidative-induced mitochondrial damage. A review, *Int. J. Hyperthermia*, 2014, **30**(7), 513–523, DOI: [10.3109/02656736.2014.971446](https://doi.org/10.3109/02656736.2014.971446).
- 104 M. Fan, L. Jia, M. Pang, X. Yang, Y. Yang, S. Kamel Elyzayati, *et al.*, Injectable Adhesive Hydrogel as Photothermal-Derived Antigen Reservoir for Enhanced Anti-Tumor Immunity, *Adv. Funct. Mater.*, 2021, **31**(20), 2010587, DOI: [10.1002/adfm.202010587](https://doi.org/10.1002/adfm.202010587).
- 105 J.-J. Fu, J.-Y. Zhang, S.-P. Li, L.-M. Zhang, Z.-X. Lin, L. Liang, *et al.*, CuS Nanodot-Loaded Thermosensitive Hydrogel for Anticancer Photothermal Therapy, *Mol. Pharm.*, 2018, **15**(10), 4621–4631, DOI: [10.1021/acs.molpharmaceut.8b00624](https://doi.org/10.1021/acs.molpharmaceut.8b00624).
- 106 J. Zeng, D. Shi, Y. Gu, T. Kaneko, L. Zhang, H. Zhang, *et al.*, Injectable and Near-Infrared-Responsive Hydrogels Encapsulating Dopamine-Stabilized Gold Nanorods with Long Photothermal Activity Controlled for Tumor Therapy, *Biomacromolecules*, 2019, **20**(9), 3375–3384, DOI: [10.1021/acs.biomac.9b00600](https://doi.org/10.1021/acs.biomac.9b00600).
- 107 H. Wang, B. Wang, S. Wang, J. Chen, W. Zhi, Y. Guan, *et al.*, Injectable in situ intelligent thermo-responsive hydrogel with glycyrrhetic acid-conjugated nano graphene oxide for chemo-photothermal therapy of malignant hepatocellular tumor, *J. Biomater. Appl.*, 2022, **37**(1), 151–165, DOI: [10.1177/08853282221078107](https://doi.org/10.1177/08853282221078107).
- 108 K. K. Lee, S. C. Lee, H. Kim and C.-S. Lee, Polydopamine Nanoparticle-Incorporated Fluorescent Hydrogel for Fluorescence Imaging-Guided Photothermal Therapy of Cancers, *BioChip J.*, 2023, **17**(1), 85–92, DOI: [10.1007/s13206-022-00091-y](https://doi.org/10.1007/s13206-022-00091-y).
- 109 E. Mei, C. Chen, C. Li, X. Ding, J. Chen, Q. Xi, *et al.*, Injectable and Biodegradable Chitosan Hydrogel-Based



- Drug Depot Contributes to Synergistic Treatment of Tumors, *Biomacromolecules*, 2021, **22**(12), 5339–5348, DOI: [10.1021/acs.biomac.1c01279](https://doi.org/10.1021/acs.biomac.1c01279).
- 110 B. Tan, Y. Wu, Y. Wu, K. Shi, R. Han, Y. Li, *et al.*, Curcumin-Microsphere/IR820 Hybrid Bifunctional Hydrogels for In Situ Osteosarcoma Chemo-co-Thermal Therapy and Bone Reconstruction, *ACS Appl. Mater. Interfaces*, 2021, **13**(27), 31542–31553, DOI: [10.1021/acsami.1c08775](https://doi.org/10.1021/acsami.1c08775).
- 111 W. He, P. Li, Y. Zhu, M. Liu, X. Huang and H. Qi, An injectable silk fibroin nanofiber hydrogel hybrid system for tumor upconversion luminescence imaging and photothermal therapy, *New J. Chem.*, 2019, **43**(5), 2213–2219, DOI: [10.1039/C8NJ05766D](https://doi.org/10.1039/C8NJ05766D).
- 112 H. Zheng and B. Zuo, Functional silk fibroin hydrogels: preparation, properties and applications, *J. Mater. Chem. B*, 2021, **9**(5), 1238–1258, DOI: [10.1039/D0TB02099K](https://doi.org/10.1039/D0TB02099K).
- 113 Y. Cao, B. Ouyang, X. Yang, Q. Jiang, L. Yu, S. Shen, *et al.*, Fixed-point “blasting” triggered by second near-infrared window light for augmented interventional photothermal therapy, *Biomater. Sci.*, 2020, **8**(10), 2955–2965, DOI: [10.1039/D0BM00372G](https://doi.org/10.1039/D0BM00372G).
- 114 C. Wei, X. Jin, C. Wu and W. Zhang, Injectable composite hydrogel based on carbon particles for photothermal therapy of bone tumor and bone regeneration, *J. Mater. Sci. Technol.*, 2022, **118**, 64–72, DOI: [10.1016/j.jmst.2021.10.053](https://doi.org/10.1016/j.jmst.2021.10.053).
- 115 X. Yang, L. Gao, Y. Wei, B. Tan, Y. Wu, C. Yi, *et al.*, Photothermal hydrogel platform for prevention of post-surgical tumor recurrence and improving breast reconstruction, *J. Nanobiotechnol.*, 2021, **19**(1), 307, DOI: [10.1186/s12951-021-01041-w](https://doi.org/10.1186/s12951-021-01041-w).
- 116 B. Liu, J. Sun, J. Zhu, B. Li, C. Ma, X. Gu, *et al.*, Injectable and NIR-Responsive DNA-Inorganic Hybrid Hydrogels with Outstanding Photothermal Therapy, *Adv. Mater.*, 2020, **32**(39), 2004460, DOI: [10.1002/adma.202004460](https://doi.org/10.1002/adma.202004460).
- 117 J. Su, S. Lu, S. Jiang, B. Li, B. Liu, Q. Sun, *et al.*, Engineered Protein Photo-Thermal Hydrogels for Outstanding In Situ Tongue Cancer Therapy, *Adv. Mater.*, 2021, **33**(21), 2100619, DOI: [10.1002/adma.202100619](https://doi.org/10.1002/adma.202100619).
- 118 X. Hu, S. Lei, S. Song, X. Xia, J. Qi, J. Liu, *et al.*, Guanosine-based Hydrogel Integrating Photothermal Effect of PDA-AuNPs through Dynamic Borate Bond for Photothermal Therapy of Cancer, *Chem. – Asian J.*, 2022, **17**(15), e202200302, DOI: [10.1002/Asia.202200302](https://doi.org/10.1002/Asia.202200302).
- 119 Y. Qi, Z. Qian, W. Yuan and Z. Li, Injectable and self-healing nanocomposite hydrogel loading needle-like nano-hydroxyapatite and graphene oxide for synergistic tumour proliferation inhibition and photothermal therapy, *J. Mater. Chem. B*, 2021, **9**(47), 9734–9743, DOI: [10.1039/D1TB01753E](https://doi.org/10.1039/D1TB01753E).
- 120 C. Wang, X. Wang, K. Dong, J. Luo, Q. Zhang and Y. Cheng, Injectable and responsively degradable hydrogel for personalized photothermal therapy, *Biomaterials*, 2016, **104**, 129–137, DOI: [10.1016/j.biomaterials.2016.07.013](https://doi.org/10.1016/j.biomaterials.2016.07.013).
- 121 H. Zheng, S. Wang, L. Zhou, X. He, Z. Cheng, F. Cheng, *et al.*, Injectable multi-responsive micelle/nanocomposite hybrid hydrogel for bioenzyme and photothermal augmented chemodynamic therapy of skin cancer and bacterial infection, *Chem. Eng. J.*, 2021, **404**, 126439, DOI: [10.1016/j.cej.2020.126439](https://doi.org/10.1016/j.cej.2020.126439).
- 122 N. Tao, Y. Liu, Y. Wu, X. Li, J. Li, X. Sun, *et al.*, Minimally Invasive Antitumor Therapy Using Biodegradable Nanocomposite Micellar Hydrogel with Functionalities of NIR-II Photothermal Ablation and Vascular Disruption, *ACS Appl. Bio Mater.*, 2020, **3**(7), 4531–4542, DOI: [10.1021/acsabm.0c00465](https://doi.org/10.1021/acsabm.0c00465).
- 123 Y. Liang, Y. Hao, Y. Wu, Z. Zhou, J. Li, X. Sun, *et al.*, Integrated Hydrogel Platform for Programmed Antitumor Therapy Based on Near Infrared-Triggered Hyperthermia and Vascular Disruption, *ACS Appl. Mater. Interfaces*, 2019, **11**(24), 21381–21390, DOI: [10.1021/acsami.9b05536](https://doi.org/10.1021/acsami.9b05536).
- 124 C. Xing, S. Chen, M. Qiu, X. Liang, Q. Liu, Q. Zou, *et al.*, Conceptually Novel Black Phosphorus/Cellulose Hydrogels as Promising Photothermal Agents for Effective Cancer Therapy, *Adv. Healthcare Mater.*, 2018, **7**(7), e1701510, DOI: [10.1002/adhm.201701510](https://doi.org/10.1002/adhm.201701510).
- 125 L. Li, C. Wang, Q. Huang, J. Xiao, Q. Zhang and Y. Cheng, A degradable hydrogel formed by dendrimer-encapsulated platinum nanoparticles and oxidized dextran for repeated photothermal cancer therapy, *J. Mater. Chem. B*, 2018, **6**(16), 2474–2480, DOI: [10.1039/C8TB00091C](https://doi.org/10.1039/C8TB00091C).
- 126 Y. Hao, Y. Liu, Y. Wu, N. Tao, D. Lou, J. Li, *et al.*, A robust hybrid nanozyme@hydrogel platform as a biomimetic cascade bioreactor for combination antitumor therapy, *Biomater. Sci.*, 2020, **8**(7), 1830–1839, DOI: [10.1039/C9BM01837A](https://doi.org/10.1039/C9BM01837A).
- 127 F. Poustchi, H. Amani, Z. Ahmadian, S. V. Niknezhad, S. Mehrabi, H. A. Santos, *et al.*, Combination Therapy of Killing Diseases by Injectable Hydrogels: From Concept to Medical Applications, *Adv. Healthcare Mater.*, 2021, **10**(3), 2001571, DOI: [10.1002/adhm.202001571](https://doi.org/10.1002/adhm.202001571).
- 128 B. Khurana, P. Gierlich, A. Meindl, L. C. Gomes-da-Silva and M. O. Senge, Hydrogels: soft matters in photomedicine, *Photochem. Photobiol. Sci.*, 2019, **18**(11), 2613–2656, DOI: [10.1039/C9PP00221A](https://doi.org/10.1039/C9PP00221A).
- 129 P. Agostinis, K. Berg, K. A. Cengel, T. H. Foster, A. W. Girotti, S. O. Gollnick, *et al.*, Photodynamic therapy of cancer: an update, *CA-Cancer J. Clin.*, 2011, **61**(4), 250–281, DOI: [10.3322/caac.20114](https://doi.org/10.3322/caac.20114).
- 130 Z. Feng, S. Lin, A. McDonagh and C. Yu, Natural Hydrogels Applied in Photodynamic Therapy, *Curr. Med. Chem.*, 2020, **27**(16), 2681–2703, DOI: [10.2174/0929867326666191016112828](https://doi.org/10.2174/0929867326666191016112828).
- 131 J.-J. Hu, Q. Lei and X.-Z. Zhang, Recent advances in photonanomedicines for enhanced cancer photodynamic therapy, *Prog. Mater. Sci.*, 2020, **114**, 100685, DOI: [10.1016/j.pmatsci.2020.100685](https://doi.org/10.1016/j.pmatsci.2020.100685).
- 132 Z. Meng, X. Zhou, J. Xu, X. Han, Z. Dong, H. Wang, *et al.*, Light-Triggered In Situ Gelation to Enable Robust Photodynamic-Immunotherapy by Repeated Stimulations,





- Adv. Mater.*, 2019, **31**(24), e1900927, DOI: [10.1002/adma.201900927](https://doi.org/10.1002/adma.201900927).
- 133 Z. Sun, X. Wang, J. Liu, Z. Wang, W. Wang, D. Kong, *et al.*, ICG/l-Arginine Encapsulated PLGA Nanoparticle-Thermosensitive Hydrogel Hybrid Delivery System for Cascade Cancer Photodynamic-NO Therapy with Promoted Collagen Depletion in Tumor Tissues, *Mol. Pharm.*, 2021, **18**(3), 928–939, DOI: [10.1021/acs.molpharmaceut.0c00937](https://doi.org/10.1021/acs.molpharmaceut.0c00937).
- 134 M. Hou, W. Liu, L. Zhang, L. Zhang, Z. Xu, Y. Cao, *et al.*, Responsive agarose hydrogel incorporated with natural humic acid and MnO<sub>2</sub> nanoparticles for effective relief of tumor hypoxia and enhanced photo-induced tumor therapy, *Biomater. Sci.*, 2020, **8**(1), 353–369, DOI: [10.1039/C9BM01472A](https://doi.org/10.1039/C9BM01472A).
- 135 T. Chen, T. Yao, H. Peng, A. K. Whittaker, Y. Li, S. Zhu, *et al.*, An Injectable Hydrogel for Simultaneous Photothermal Therapy and Photodynamic Therapy with Ultrahigh Efficiency Based on Carbon Dots and Modified Cellulose Nanocrystals, *Adv. Funct. Mater.*, 2021, **31**(45), 2106079, DOI: [10.1002/adfm.202106079](https://doi.org/10.1002/adfm.202106079).
- 136 J. Sun, Y. Guo, R. Xing, T. Jiao, Q. Zou and X. Yan, Synergistic in vivo photodynamic and photothermal anti-tumor therapy based on collagen-gold hybrid hydrogels with inclusion of photosensitive drugs, *Colloids Surf., A*, 2017, **514**, 155–160, DOI: [10.1016/j.colsurfa.2016.11.062](https://doi.org/10.1016/j.colsurfa.2016.11.062).
- 137 C. Liu, C. Ruan, R. Shi, B. P. Jiang, S. Ji and X. C. Shen, A near infrared-modulated thermosensitive hydrogel for stabilization of indocyanine green and combinatorial anti-cancer phototherapy, *Biomater. Sci.*, 2019, **7**(4), 1705–1715, DOI: [10.1039/c8bm01541d](https://doi.org/10.1039/c8bm01541d).
- 138 R. Xing, K. Liu, T. Jiao, N. Zhang, K. Ma, R. Zhang, *et al.*, An Injectable Self-Assembling Collagen-Gold Hybrid Hydrogel for Combinatorial Antitumor Photothermal/Photodynamic Therapy, *Adv. Mater.*, 2016, **28**(19), 3669–3676, DOI: [10.1002/adma.201600284](https://doi.org/10.1002/adma.201600284).
- 139 Y. Qi, Y. Yuan, Z. Qian, X. Ma, W. Yuan and Y. Song, Injectable and Self-Healing Polysaccharide Hydrogel Loading Molybdenum Disulfide Nanoflakes for Synergistic Photothermal-Photodynamic Therapy of Breast Cancer, *Macromol. Biosci.*, 2022, **22**(9), 2200161, DOI: [10.1002/mabi.202200161](https://doi.org/10.1002/mabi.202200161).
- 140 R. Jin, X. Yang, D. Zhao, X. Hou, C. Li, X. Song, *et al.*, An injectable hybrid hydrogel based on a genetically engineered polypeptide for second near-infrared fluorescence/photoacoustic imaging-monitored sustained chemophotothermal therapy, *Nanoscale*, 2019, **11**(34), 16080–16091, DOI: [10.1039/C9NR04630E](https://doi.org/10.1039/C9NR04630E).
- 141 Y.-W. Jiang, G. Gao, P. Hu, J.-B. Liu, Y. Guo, X. Zhang, *et al.*, Palladium nanosheet-knotted injectable hydrogels formed via palladium–sulfur bonding for synergistic chemo-photothermal therapy, *Nanoscale*, 2020, **12**(1), 210–219, DOI: [10.1039/C9NR08454A](https://doi.org/10.1039/C9NR08454A).
- 142 Z. Zhao, H. Zhang, H. Chen, Y. Xu, L. Ma and Z. Wang, An efficient photothermal-chemotherapy platform based on a polyacrylamide/phytic acid/polydopamine hydrogel, *J. Mater. Chem. B*, 2022, **10**(21), 4012–4019, DOI: [10.1039/d2tb00677d](https://doi.org/10.1039/d2tb00677d).
- 143 N. Zhang, X. Xu, X. Zhang, D. Qu, L. Xue, R. Mo, *et al.*, Nanocomposite hydrogel incorporating gold nanorods and paclitaxel-loaded chitosan micelles for combination photothermal-chemotherapy, *Int. J. Pharm.*, 2016, **497**(1–2), 210–221, DOI: [10.1016/j.ijpharm.2015.11.032](https://doi.org/10.1016/j.ijpharm.2015.11.032).
- 144 J. Zhou, M. Wang, Y. Han, J. Lai and J. Chen, Multistage-Targeted Gold/Mesoporous Silica Nanocomposite Hydrogel as In Situ Injectable Drug Release System for Chemophotothermal Synergistic Cancer Therapy, *ACS Appl. Bio Mater.*, 2020, **3**(1), 421–431, DOI: [10.1021/acsabm.9b00895](https://doi.org/10.1021/acsabm.9b00895).
- 145 G. Wang, N. Zhang, Z. Cao, Z. Zhang, Z. Zhu, G. Sun, *et al.*, Injectable hydrogel-mediated combination of hyperthermia ablation and photo-enhanced chemotherapy in the NIR-II window for tumor eradication, *Biomater. Sci.*, 2021, **9**(9), 3516–3525, DOI: [10.1039/D1BM00371B](https://doi.org/10.1039/D1BM00371B).
- 146 R. Jin, J. Yang, D. Zhao, X. Hou, C. Li, W. Chen, *et al.*, Hollow gold nanoshells-incorporated injectable genetically engineered hydrogel for sustained chemo-photothermal therapy of tumor, *J. Nanobiotechnol.*, 2019, **17**(1), 99, DOI: [10.1186/s12951-019-0532-9](https://doi.org/10.1186/s12951-019-0532-9).
- 147 X. Men, H. Chen, C. Sun, Y. Liu, R. Wang, X. Zhang, *et al.*, Thermosensitive Polymer Dot Nanocomposites for Trimodal Computed Tomography/Photoacoustic/Fluorescence Imaging-Guided Synergistic Chemo-Photothermal Therapy, *ACS Appl. Mater. Interfaces*, 2020, **12**(46), 51174–51184, DOI: [10.1021/acsami.0c13252](https://doi.org/10.1021/acsami.0c13252).
- 148 P. Hu, W. Wang, J. Sha, Y. Xing, Y. Wang, C. Wu, *et al.*, Tumor microenvironment responsive-multifunctional nanocomposites knotted injectable hydrogels for enhanced synergistic chemodynamic and chemo-photothermal therapies, *Mater. Des.*, 2023, **225**, 111429, DOI: [10.1016/j.matdes.2022.111429](https://doi.org/10.1016/j.matdes.2022.111429).
- 149 Y. Wu, Y. Liang, Y. Liu, Y. Hao, N. Tao, J. Li, *et al.*, A Bi2S3-embedded gellan gum hydrogel for localized tumor photothermal/antiangiogenic therapy, *J. Mater. Chem. B*, 2021, **9**(14), 3224–3234, DOI: [10.1039/D1TB00257K](https://doi.org/10.1039/D1TB00257K).
- 150 C. Ruan, C. Liu, H. Hu, X.-L. Guo, B.-P. Jiang, H. Liang, *et al.*, NIR-II light-modulated thermosensitive hydrogel for light-triggered cisplatin release and repeatable chemophotothermal therapy, *Chem. Sci.*, 2019, **10**(17), 4699–4706, DOI: [10.1039/C9SC00375D](https://doi.org/10.1039/C9SC00375D).
- 151 S. Geng, H. Zhao, G. Zhan, Y. Zhao and X. Yang, Injectable in Situ Forming Hydrogels of Thermosensitive Polypyrrole Nanoplatforams for Precisely Synergistic Photothermo-Chemotherapy, *ACS Appl. Mater. Interfaces*, 2020, **12**(7), 7995–8005, DOI: [10.1021/acsami.9b22654](https://doi.org/10.1021/acsami.9b22654).
- 152 S. Luo, J. Wu, Z. Jia, P. Tang, J. Sheng, C. Xie, *et al.*, An Injectable, Bifunctional Hydrogel with Photothermal Effects for Tumor Therapy and Bone Regeneration, *Macromol. Biosci.*, 2019, **19**(9), e1900047, DOI: [10.1002/mabi.201900047](https://doi.org/10.1002/mabi.201900047).
- 153 J. Zhao, J. Li, C. Zhu, F. Hu, H. Wu, X. Man, *et al.*, Design of Phase-Changeable and Injectable Alginate Hydrogel for





- Imaging-Guided Tumor Hyperthermia and Chemotherapy, *ACS Appl. Mater. Interfaces*, 2018, **10**(4), 3392–3404, DOI: [10.1021/acsami.7b17608](https://doi.org/10.1021/acsami.7b17608).
- 154 X. Zhu, Y. Zhang, H. Huang, H. Zhang, L. Hou and Z. Zhang, Functionalized graphene oxide-based thermo-sensitive hydrogel for near-infrared chemo-photothermal therapy on tumor, *J. Biomater. Appl.*, 2016, **30**(8), 1230–1241, DOI: [10.1177/0885328215619583](https://doi.org/10.1177/0885328215619583).
- 155 A. Zheng, D. Wu, M. Fan, H. Wang, Y. Liao, Q. Wang, *et al.*, Injectable zwitterionic thermosensitive hydrogels with low-protein adsorption and combined effect of photothermal-chemotherapy, *J. Mater. Chem. B*, 2020, **8**(46), 10637–10649, DOI: [10.1039/D0TB01763A](https://doi.org/10.1039/D0TB01763A).
- 156 J. Chen, H. Gu, S. Fu, J. Lu, H. Tan, Q. Wei, *et al.*, Multifunctional injectable hydrogels for three-in-one cancer therapy: Preoperative remission via mild photothermal-enhanced supramolecular chemotherapy and prevention of postoperative recurrence and adhesion, *Chem. Eng. J.*, 2021, **425**, 130377, DOI: [10.1016/j.cej.2021.130377](https://doi.org/10.1016/j.cej.2021.130377).
- 157 M. Yang, S. Y. Lee, S. Kim, J. S. Koo, J. H. Seo, D. I. Jeong, *et al.*, Selenium and dopamine-crosslinked hyaluronic acid hydrogel for chemophotothermal cancer therapy, *J. Controlled Release*, 2020, **324**, 750–764, DOI: [10.1016/j.jconrel.2020.04.024](https://doi.org/10.1016/j.jconrel.2020.04.024).
- 158 L. Qin, G. Ling, F. Peng, F. Zhang, S. Jiang, H. He, *et al.*, Black phosphorus nanosheets and gemcitabine encapsulated thermo-sensitive hydrogel for synergistic photothermal-chemotherapy, *J. Colloid Interface Sci.*, 2019, **556**, 232–238, DOI: [10.1016/j.jcis.2019.08.058](https://doi.org/10.1016/j.jcis.2019.08.058).
- 159 S. Sang, Z. Jiang, N. Xie, H. Rao, K. Liao, Q. Hu, *et al.*, Black phosphorus nanosheets and paclitaxel encapsulated hydrogel for synergistic photothermal-chemotherapy, *Nanophotonics*, 2021, **10**(10), 2625–2637, DOI: [10.1515/nanoph-2021-0089](https://doi.org/10.1515/nanoph-2021-0089).
- 160 P. Sun, T. Huang, X. Wang, G. Wang, Z. Liu, G. Chen, *et al.*, Dynamic-Covalent Hydrogel with NIR-Triggered Drug Delivery for Localized Chemo-Photothermal Combination Therapy, *Biomacromolecules*, 2020, **21**(2), 556–565, DOI: [10.1021/acs.biomac.9b01290](https://doi.org/10.1021/acs.biomac.9b01290).
- 161 X. Wang, C. Wang, X. Wang, Y. Wang, Q. Zhang and Y. Cheng, A Polydopamine Nanoparticle-Knotted Poly (ethylene glycol) Hydrogel for On-Demand Drug Delivery and Chemo-photothermal Therapy, *Chem. Mater.*, 2017, **29**(3), 1370–1376, DOI: [10.1021/acs.chemmater.6b05192](https://doi.org/10.1021/acs.chemmater.6b05192).
- 162 M. Liu, P. Huang, W. Wang, Z. Feng, J. Zhang, L. Deng, *et al.*, An injectable nanocomposite hydrogel co-constructed with gold nanorods and paclitaxel-loaded nanoparticles for local chemo-photothermal synergistic cancer therapy, *J. Mater. Chem. B*, 2019, **7**(16), 2667–2677, DOI: [10.1039/C9TB00120D](https://doi.org/10.1039/C9TB00120D).
- 163 B. Wang, S. Wu, Z. Lin, Y. Jiang, Y. Chen, Z. S. Chen, *et al.*, A personalized and long-acting local therapeutic platform combining photothermal therapy and chemotherapy for the treatment of multidrug-resistant colon tumor, *Int. J. Nanomed.*, 2018, **13**, 8411–8427, DOI: [10.2147/ij.n.s184728](https://doi.org/10.2147/ij.n.s184728).
- 164 C. Wang, N. Zhao and W. Yuan, NIR/Thermoresponsive Injectable Self-Healing Hydrogels Containing Polydopamine Nanoparticles for Efficient Synergistic Cancer Thermochemotherapy, *ACS Appl. Mater. Interfaces*, 2020, **12**(8), 9118–9131, DOI: [10.1021/acsami.9b23536](https://doi.org/10.1021/acsami.9b23536).
- 165 X. Xu, Z. Huang, Z. Huang, X. Zhang, S. He, X. Sun, *et al.*, Injectable, NIR/pH-Responsive Nanocomposite Hydrogel as Long-Acting Implant for Chemophotothermal Synergistic Cancer Therapy, *ACS Appl. Mater. Interfaces*, 2017, **9**(24), 20361–20375, DOI: [10.1021/acsami.7b02307](https://doi.org/10.1021/acsami.7b02307).
- 166 L. Rong, Y. Liu, Y. Fan, J. Xiao, Y. Su, L. Lu, *et al.*, Injectable nano-composite hydrogels based on hyaluronic acid-chitosan derivatives for simultaneous photothermal-chemo therapy of cancer with anti-inflammatory capacity, *Carbohydr. Polym.*, 2023, **310**, 120721, DOI: [10.1016/j.carbpol.2023.120721](https://doi.org/10.1016/j.carbpol.2023.120721).
- 167 Z. Qian, N. Zhao, C. Wang and W. Yuan, Injectable self-healing polysaccharide hydrogel loading CuS and pH-responsive DOX@ZIF-8 nanoparticles for synergistic photothermal-photodynamic-chemo therapy of cancer, *J. Mater. Sci. Technol.*, 2022, **127**, 245–255, DOI: [10.1016/j.jmst.2022.04.015](https://doi.org/10.1016/j.jmst.2022.04.015).
- 168 J. Yang, Z. Sun, Q. Dou, S. Hui, P. Zhang, R. Liu, *et al.*, NIR-light-responsive chemo-photothermal hydrogel system with controlled DOX release and photothermal effect for cancer therapy, *Colloids Surf., A*, 2023, **667**, 131407, DOI: [10.1016/j.colsurfa.2023.131407](https://doi.org/10.1016/j.colsurfa.2023.131407).
- 169 V. Revuri, S. K. Rajendrakumar, M. S. Park, A. Mohapatra, S. Uthaman, J. Mondal, *et al.*, Heat-Confined Tumor-Docking Reversible Thermogel Potentiates Systemic Antitumor Immune Response During Near-Infrared Photothermal Ablation in Triple-Negative Breast Cancer, *Adv. Healthcare Mater.*, 2021, **10**(21), e2100907, DOI: [10.1002/adhm.202100907](https://doi.org/10.1002/adhm.202100907).
- 170 E. Mei, S. Li, J. Song, R. Xing, Z. Li and X. Yan, Self-assembling Collagen/Alginate hybrid hydrogels for combinatorial photothermal and immuno tumor therapy, *Colloids Surf., A*, 2019, **577**, 570–575, DOI: [10.1016/j.colsurfa.2019.06.023](https://doi.org/10.1016/j.colsurfa.2019.06.023).
- 171 W. Zhang, S. Li, Y. Liu, R. Xing, Z. Jin, X. Yan, *et al.*, Immunosuppressive microenvironment improvement and treatment of aggressive malignancy pancreatic ductal adenocarcinoma based on local administration of injectable hydrogel, *Nano Today*, 2023, **50**, 101832, DOI: [10.1016/j.nantod.2023.101832](https://doi.org/10.1016/j.nantod.2023.101832).
- 172 Y. P. Jia, K. Shi, F. Yang, J. F. Liao, R. X. Han, L. P. Yuan, *et al.*, Multifunctional Nanoparticle Loaded Injectable Thermoresponsive Hydrogel as NIR Controlled Release Platform for Local Photothermal Immunotherapy to Prevent Breast Cancer Postoperative Recurrence and Metastases, *Adv. Funct. Mater.*, 2020, **30**(25), 2001059, DOI: [10.1002/adfm.202001059](https://doi.org/10.1002/adfm.202001059).
- 173 Z. Wang, W. Zeng, Z. Chen, W. Suo, H. Quan and Z. J. Tan, An intratumoral injectable nanozyme hydrogel for hypoxia-resistant thermoradiotherapy, *Colloids Surf., B*, 2021, **207**, 112026, DOI: [10.1016/j.colsurfb.2021.112026](https://doi.org/10.1016/j.colsurfb.2021.112026).



- 174 R. Jin, J. Yang, P. Ding, C. Li, B. Zhang, W. Chen, *et al.*, Antitumor immunity triggered by photothermal therapy and photodynamic therapy of a 2D MoS<sub>2</sub> nanosheet-incorporated injectable polypeptide-engineered hydrogel combined with chemotherapy for 4T1 breast tumor therapy, *Nanotechnology*, 2020, **31**(20), 205102, DOI: [10.1088/1361-6528/ab72b9](https://doi.org/10.1088/1361-6528/ab72b9).
- 175 H. Zhang, X. Zhu, Y. Ji, X. Jiao, Q. Chen, L. Hou, *et al.*, Near-infrared-triggered in situ hybrid hydrogel system for synergistic cancer therapy, *J. Mater. Chem. B*, 2015, **3**(30), 6310–6326, DOI: [10.1039/c5tb00904a](https://doi.org/10.1039/c5tb00904a).
- 176 Y. Wu, F. Chen, N. Huang, J. Li, C. Wu, B. Tan, *et al.*, Near-infrared light-responsive hybrid hydrogels for the synergistic chemo-photothermal therapy of oral cancer, *Nanoscale*, 2021, **13**(40), 17168–17182, DOI: [10.1039/d1nr04625j](https://doi.org/10.1039/d1nr04625j).
- 177 X. L. Hou, X. Dai, J. Yang, B. Zhang, D. H. Zhao, C. Q. Li, *et al.*, Injectable polypeptide-engineered hydrogel depot for amplifying the anti-tumor immune effect induced by chemo-photothermal therapy, *J. Mater. Chem. B*, 2020, **8**(37), 8623–8633, DOI: [10.1039/d0tb01370f](https://doi.org/10.1039/d0tb01370f).
- 178 J. Zhang, L. Yang, F. Huang, C. Zhao, J. Liu, Y. Zhang, *et al.*, Multifunctional Hybrid Hydrogel Enhanced Antitumor Therapy through Multiple Destroying DNA Functions by a Triple-Combination Synergistic Therapy, *Adv. Healthcare Mater.*, 2021, **10**(21), e2101190, DOI: [10.1002/adhm.202101190](https://doi.org/10.1002/adhm.202101190).
- 179 Z. Shen, Q. Ma, X. Zhou, G. Zhang, G. Hao, Y. Sun, *et al.*, Strategies to improve photodynamic therapy efficacy by relieving the tumor hypoxia environment, *NPG Asia Mater.*, 2021, **13**(1), 39, DOI: [10.1038/s41427-021-00303-1](https://doi.org/10.1038/s41427-021-00303-1).
- 180 D. Hu, M. Pan, Y. Yu, A. Sun, K. Shi, Y. Qu, *et al.*, Application of nanotechnology for enhancing photodynamic therapy via ameliorating, neglecting, or exploiting tumor hypoxia, *View*, 2020, **1**(1), e6, DOI: [10.1002/viw2.6](https://doi.org/10.1002/viw2.6).
- 181 Z. Tang, P. Zhao, D. Ni, Y. Liu, M. Zhang, H. Wang, *et al.*, Pyroelectric nanoplatform for NIR-II-triggered photothermal therapy with simultaneous pyroelectric dynamic therapy, *Mater. Horiz.*, 2018, **5**(5), 946–952, DOI: [10.1039/C8MH00627J](https://doi.org/10.1039/C8MH00627J).
- 182 J. Wang, X. Wu, P. Shen, J. Wang, Y. Shen, Y. Shen, *et al.*, Applications of Inorganic Nanomaterials in Photothermal Therapy Based on Combinational Cancer Treatment, *Int. J. Nanomed.*, 2020, **15**, 1903–1914, DOI: [10.2147/ijn.s239751](https://doi.org/10.2147/ijn.s239751).
- 183 C. Fiorica, F. S. Palumbo, G. Pitarresi, R. Puleio, L. Condorelli, G. Collura, *et al.*, A hyaluronic acid/cyclodextrin based injectable hydrogel for local doxorubicin delivery to solid tumors, *Int. J. Pharm.*, 2020, **589**, 119879, DOI: [10.1016/j.ijpharm.2020.119879](https://doi.org/10.1016/j.ijpharm.2020.119879).
- 184 Y. Xiao, Y. Gu, L. Qin, L. Chen, X. Chen, W. Cui, *et al.*, Injectable thermosensitive hydrogel-based drug delivery system for local cancer therapy, *Colloids Surf., B*, 2021, **200**, 111581, DOI: [10.1016/j.colsurfb.2021.111581](https://doi.org/10.1016/j.colsurfb.2021.111581).
- 185 X. Huang, Y. Lu, M. Guo, S. Du and N. Han, Recent strategies for nano-based PTT combined with immunotherapy: from a biomaterial point of view, *Theranostics*, 2021, **11**(15), 7546–7569, DOI: [10.7150/thno.56482](https://doi.org/10.7150/thno.56482).
- 186 R. Lima-Sousa, B. L. Melo, C. G. Alves, A. F. Moreira, A. G. Mendonça, I. J. Correia, *et al.*, Combining Photothermal-Photodynamic Therapy Mediated by Nanomaterials with Immune Checkpoint Blockade for Metastatic Cancer Treatment and Creation of Immune Memory, *Adv. Funct. Mater.*, 2021, **31**(29), 2010777, DOI: [10.1002/adfm.202010777](https://doi.org/10.1002/adfm.202010777).
- 187 T. Shang, X. Yu, S. Han and B. Yang, Nanomedicine-based tumor photothermal therapy synergized immunotherapy, *Biomater. Sci.*, 2020, **8**(19), 5241–5259, DOI: [10.1039/D0BM01158D](https://doi.org/10.1039/D0BM01158D).
- 188 C. G. Alves, R. Lima-Sousa, B. L. Melo, A. F. Moreira, I. J. Correia and D. de Melo-Diogo, Heptamethine Cyanine-Loaded Nanomaterials for Cancer Immuno-Photothermal/Photodynamic Therapy: A Review, *Pharmaceutics*, 2022, **14**(5), 1015, DOI: [10.3390/pharmaceutics14051015](https://doi.org/10.3390/pharmaceutics14051015).
- 189 Z. Shen, J. Xia, Q. Ma, W. Zhu, Z. Gao, S. Han, *et al.*, Tumor Microenvironment-triggered Nanosystems as dual-relief Tumor Hypoxia Immunomodulators for enhanced Phototherapy, *Theranostics*, 2020, **10**(20), 9132–9152, DOI: [10.7150/thno.46076](https://doi.org/10.7150/thno.46076).
- 190 Z. Wang, B. Guo, E. Middha, Z. Huang, Q. Hu, Z. Fu, *et al.*, Microfluidics-Prepared Uniform Conjugated Polymer Nanoparticles for Photo-Triggered Immune Microenvironment Modulation and Cancer Therapy, *ACS Appl. Mater. Interfaces*, 2019, **11**(12), 11167–11176, DOI: [10.1021/acsami.8b22579](https://doi.org/10.1021/acsami.8b22579).
- 191 P. Xu and F. Liang, Nanomaterial-Based Tumor Photothermal Immunotherapy, *Int. J. Nanomed.*, 2020, **15**, 9159–9180, DOI: [10.2147/ijn.s249252](https://doi.org/10.2147/ijn.s249252).
- 192 D. Liu, B. Chen, Y. Mo, Z. Wang, T. Qi, Q. Zhang, *et al.*, Redox-Activated Porphyrin-Based Liposome Remote-Loaded with Indoleamine 2,3-Dioxygenase (IDO) Inhibitor for Synergistic Photoimmunotherapy through Induction of Immunogenic Cell Death and Blockage of IDO Pathway, *Nano Lett.*, 2019, **19**(10), 6964–6976, DOI: [10.1021/acs.nanolett.9b02306](https://doi.org/10.1021/acs.nanolett.9b02306).
- 193 Q. Chen, L. Xu, C. Liang, C. Wang, R. Peng and Z. Liu, Photothermal therapy with immune-adjuvant nanoparticles together with checkpoint blockade for effective cancer immunotherapy, *Nat. Commun.*, 2016, **7**, 13193, DOI: [10.1038/ncomms13193](https://doi.org/10.1038/ncomms13193).
- 194 Y. Chao, Q. Chen and Z. Liu, Smart Injectable Hydrogels for Cancer Immunotherapy, *Adv. Funct. Mater.*, 2020, **30**(2), 1902785, DOI: [10.1002/adfm.201902785](https://doi.org/10.1002/adfm.201902785).
- 195 J. Liu, Y. Zhang, Q. Li, Z. Feng, P. Huang, W. Wang, *et al.*, Development of injectable thermosensitive polypeptide hydrogel as facile radioisotope and radiosensitizer hotspot for synergistic brachytherapy, *Acta Biomater.*, 2020, **114**, 133–145, DOI: [10.1016/j.actbio.2020.07.032](https://doi.org/10.1016/j.actbio.2020.07.032).
- 196 Y. Chao, L. Xu, C. Liang, L. Feng, J. Xu, Z. Dong, *et al.*, Combined local immunostimulatory radioisotope therapy and systemic immune checkpoint blockade imparts potent antitumour responses, *Nat. Biomed. Eng.*, 2018, **2**(8), 611–621, DOI: [10.1038/s41551-018-0262-6](https://doi.org/10.1038/s41551-018-0262-6).



- 197 S. Correa, A. K. Grosskopf, H. Lopez Hernandez, D. Chan, A. C. Yu, L. M. Stapleton, *et al.*, Translational Applications of Hydrogels, *Chem. Rev.*, 2021, **121**(18), 11385–11457, DOI: [10.1021/acs.chemrev.0c01177](https://doi.org/10.1021/acs.chemrev.0c01177).
- 198 Y. Yong, X. Cheng, T. Bao, M. Zu, L. Yan, W. Yin, *et al.*, Tungsten Sulfide Quantum Dots as Multifunctional Nanotheranostics for In Vivo Dual-Modal Image-Guided Photothermal/Radiotherapy Synergistic Therapy, *ACS Nano*, 2015, **9**(12), 12451–12463, DOI: [10.1021/acs.nano.5b05825](https://doi.org/10.1021/acs.nano.5b05825).
- 199 Z. Xie, T. Fan, J. An, W. Choi, Y. Duo, Y. Ge, *et al.*, Emerging combination strategies with phototherapy in cancer nanomedicine, *Chem. Soc. Rev.*, 2020, **49**(22), 8065–8087, DOI: [10.1039/D0CS00215A](https://doi.org/10.1039/D0CS00215A).
- 200 A. Szasz, Heterogeneous Heat Absorption Is Complementary to Radiotherapy, *Cancers*, 2022, **14**(4), 901, DOI: [10.3390/cancers14040901](https://doi.org/10.3390/cancers14040901).
- 201 Hydrogel Market by Raw Material Type, Composition, Form, Product, and End-User: Global Opportunity Analysis and Industry Forecast 2020–2027. Available from: <https://www.alliedmarketresearch.com/hydrogel-market>.
- 202 S. Cascone and G. Lamberti, Hydrogel-based commercial products for biomedical applications: A review, *Int. J. Pharm.*, 2020, **573**, 118803, DOI: [10.1016/j.ijpharm.2019.118803](https://doi.org/10.1016/j.ijpharm.2019.118803).
- 203 I. Mó, I. J. Sabino, D. Melo-Diogo, R. Lima-Sousa, C. G. Alves and I. J. Correia, The importance of spheroids in analyzing nanomedicine efficacy, *Nanomedicine*, 2020, **15**(15), 1513–1525, DOI: [10.2217/nmm-2020-0054](https://doi.org/10.2217/nmm-2020-0054).
- 204 C. Probst, S. Schneider and P. Loskill, High-throughput organ-on-a-chip systems: Current status and remaining challenges, *Curr. Opin. Biomed. Eng.*, 2018, **6**, 33–41, DOI: [10.1016/j.cobme.2018.02.004](https://doi.org/10.1016/j.cobme.2018.02.004).

